Experimental Studies of SF_6-CF_4 Mixtures for use as Gaseous Dielectrics in Power System Applications

By

Jeffrey Melvin Berg

May, 1995

A thesis presented to
The University of Manitoba
in fulfilment of the thesis requirement for the degree of
Master of Science
in
Electrical and Computer Engineering

Winnipeg, Manitoba
Canada

ISBN 0-612-12980-2

Name Jeffrey Melvin Berg

Dissertation Abstracts International is arranged by broad, general subject categories. Please select the one subject which most nearly describes the content of your dissertation. Enter the corresponding four-digit code in the spaces provided.

Power Systems/High Voltage Engineering
SUBJECT TERM

0544
SUBJECT CODE

U·M·I

Subject Categories

THE HUMANITIES AND SOCIAL SCIENCES

COMMUNICATIONS AND THE ARTS
- Architecture 0729
- Art History 0377
- Cinema 0900
- Dance 0378
- Fine Arts 0357
- Information Science 0723
- Journalism 0391
- Library Science 0399
- Mass Communications 0708
- Music 0413
- Speech Communication 0459
- Theater 0465

EDUCATION
- General 0515
- Administration 0514
- Adult and Continuing 0516
- Agricultural 0517
- Art 0273
- Bilingual and Multicultural 0282
- Business 0688
- Community College 0275
- Curriculum and Instruction 0727
- Early Childhood 0518
- Elementary 0524
- Finance 0277
- Guidance and Counseling 0519
- Health 0680
- Higher 0745
- History of 0520
- Home Economics 0278
- Industrial 0521
- Language and Literature 0279
- Mathematics 0280
- Music 0522
- Philosophy of 0998
- Physical 0523
- Psychology 0525
- Reading 0535
- Religious 0527
- Sciences 0714
- Secondary 0533
- Social Sciences 0534
- Sociology of 0340
- Special 0529
- Teacher Training 0530
- Technology 0710
- Tests and Measurements 0288
- Vocational 0747

LANGUAGE, LITERATURE AND LINGUISTICS
- Language
  - General 0679
  - Ancient 0289
  - Linguistics 0290
  - Modern 0291
- Literature
  - General 0401
  - Classical 0294
  - Comparative 0295
  - Medieval 0297
  - Modern 0298
  - African 0316
  - American 0591
  - Asian 0305
  - Canadian (English) 0352
  - Canadian (French) 0355
  - English 0593
  - Germanic 0311
  - Latin American 0312
  - Middle Eastern 0315
  - Romance 0313
  - Slavic and East European 0314

PHILOSOPHY, RELIGION AND THEOLOGY
- Philosophy 0422
- Religion
  - General 0318
  - Biblical Studies 0321
  - Clergy 0319
  - History of 0320
  - Philosophy of 0322
- Theology 0469

SOCIAL SCIENCES
- American Studies 0323
- Anthropology
  - Archaeology 0324
  - Cultural 0326
  - Physical 0327
- Business Administration
  - General 0310
  - Accounting 0272
  - Banking 0770
  - Management 0454
  - Marketing 0338
- Canadian Studies 0385
- Economics
  - General 0501
  - Agricultural 0503
  - Commerce-Business 0505
  - Finance 0508
  - History 0509
  - Labor 0510
  - Theory 0511
- Folklore 0358
- Geography 0366
- Gerontology 0351
- History
  - General 0578
  - Ancient 0579
  - Medieval 0581
  - Modern 0582
  - Black 0328
  - African 0331
  - Asia, Australia and Oceania 0332
  - Canadian 0334
  - European 0335
  - Latin American 0336
  - Middle Eastern 0333
  - United States 0337
- History of Science 0585
- Law 0398
- Political Science
  - General 0615
  - International Law and Relations 0616
  - Public Administration 0617
- Recreation 0814
- Social Work 0452
- Sociology
  - General 0626
  - Criminology and Penology 0627
  - Demography 0938
  - Ethnic and Racial Studies 0631
  - Individual and Family Studies 0628
  - Industrial and Labor Relations 0629
  - Public and Social Welfare 0630
  - Social Structure and Development 0700
  - Theory and Methods 0344
- Transportation 0709
- Urban and Regional Planning 0999
- Women's Studies 0453

THE SCIENCES AND ENGINEERING

BIOLOGICAL SCIENCES
- Agriculture
  - General 0473
  - Agronomy 0285
  - Animal Culture and Nutrition 0475
  - Animal Pathology 0476
  - Food Science and Technology 0359
  - Forestry and Wildlife 0478
  - Plant Culture 0479
  - Plant Pathology 0480
  - Plant Physiology 0817
  - Range Management 0777
  - Wood Technology 0746
- Biology
  - General 0306
  - Anatomy 0287
  - Biostatistics 0308
  - Botany 0309
  - Cell 0379
  - Ecology 0329
  - Entomology 0353
  - Genetics 0369
  - Limnology 0793
  - Microbiology 0410
  - Molecular 0307
  - Neuroscience 0317
  - Oceanography 0416
  - Physiology 0433
  - Radiation 0821
  - Veterinary Science 0778
  - Zoology 0472
- Biophysics
  - General 0786
  - Medical 0760

EARTH SCIENCES
- Biogeochemistry 0425
- Geochemistry 0996
- Geodesy 0370
- Geology 0372
- Geophysics 0373
- Hydrology 0388
- Mineralogy 0411
- Paleobotany 0345
- Paleoecology 0426
- Paleontology 0418
- Paleozoology 0985
- Palynology 0427
- Physical Geography 0368
- Physical Oceanography 0415

HEALTH AND ENVIRONMENTAL SCIENCES
- Environmental Sciences 0768
- Health Sciences
  - General 0566
  - Audiology 0300
  - Chemotherapy 0992
  - Dentistry 0567
  - Education 0350
  - Hospital Management 0769
  - Human Development 0758
  - Immunology 0982
  - Medicine and Surgery 0564
  - Mental Health 0347
  - Nursing 0569
  - Nutrition 0570
  - Obstetrics and Gynecology 0380
  - Occupational Health and Therapy 0354
  - Ophthalmology 0381
  - Pathology 0571
  - Pharmacology 0419
  - Pharmacy 0572
  - Physical Therapy 0382
  - Public Health 0573
  - Radiology 0574
  - Recreation 0575
  - Speech Pathology 0460
  - Toxicology 0383
- Home Economics 0386

PHYSICAL SCIENCES
Pure Sciences
- Chemistry
  - General 0485
  - Agricultural 0749
  - Analytical 0486
  - Biochemistry 0487
  - Inorganic 0488
  - Nuclear 0738
  - Organic 0490
  - Pharmaceutical 0491
  - Physical 0494
  - Polymer 0495
  - Radiation 0754
- Mathematics 0405
- Physics
  - General 0605
  - Acoustics 0986
  - Astronomy and Astrophysics 0606
  - Atmospheric Science 0608
  - Atomic 0748
  - Electronics and Electricity 0607
  - Elementary Particles and High Energy 0798
  - Fluid and Plasma 0759
  - Molecular 0609
  - Nuclear 0610
  - Optics 0752
  - Radiation 0756
  - Solid State 0611
- Statistics 0463

Applied Sciences
- Applied Mechanics 0346
- Computer Science 0984
- Engineering
  - General 0537
  - Aerospace 0538
  - Agricultural 0539
  - Automotive 0540
  - Biomedical 0541
  - Chemical 0542
  - Civil 0543
  - Electronics and Electrical 0544
  - Heat and Thermodynamics 0348
  - Hydraulic 0545
  - Industrial 0546
  - Marine 0547
  - Materials Science 0794
  - Mechanical 0548
  - Metallurgy 0743
  - Mining 0551
  - Nuclear 0552
  - Packaging 0549
  - Petroleum 0765
  - Sanitary and Municipal 0554
  - System Science 0790
- Geotechnology 0428
- Operations Research 0796
- Plastics Technology 0795
- Textile Technology 0994

PSYCHOLOGY
- General 0621
- Behavioral 0384
- Clinical 0622
- Developmental 0620
- Experimental 0623
- Industrial 0624
- Personality 0625
- Physiological 0989
- Psychobiology 0349
- Psychometrics 0632
- Social 0451

EXPERIMENTAL STUDIES OF SF_6-CF_4 MIXTURES FOR USE AS GASEOUS DIELECTRICS IN POWER SYSTEM APPLICATIONS

BY

JEFFREY MELVIN BERG

A Thesis submitted to the Faculty of Graduate Studies of the University of Manitoba in partial fulfillment of the requirements of the degree of

MASTER OF SCIENCE

Acknowledgements

I would like to take this opportunity to express my sincere gratitude to my advisor Dr. Edmund Kuffel for his steadfast guidance and support during the course of this work. His prodigious knowledge of gaseous dielectric phenomena and atomic physics was an immense asset to me. Special thanks must also be extended to Dr. Maddakere Raghuveer whose proficiency in high voltage techniques and expert opinion on many engineering related problems were of invaluable assistance. I also wish to acknowledge the efforts of Mr. John Kendall and Mr. Gordon Toole for providing the much appreciated technical assistance and support during the experimental phase of my research. Finally, I must graciously thank Manitoba Hydro and the National Science and Engineering Research Council of Canada for the financial support that made this Master of Science Thesis possible.

Abstract

Binary gas mixtures consisting of sulphurhexafluoride (SF_6) and carbontetrafluoride (CF_4) have been used for several years in the design of electrical gas insulated switchgear manufactured for operation in geographic regions of extremely low temperature. CF_4, which has a liquifaction temperature comparable to that of nitrogen (N_2) greatly reduces the risk of liquifaction and the loss of insulation of electrical equipment when mixed with SF_6 at practical pressures (200-400 kPa). In addition, SF_6-CF_4 mixtures offer better arc quenching properties than those displayed by SF_6-N_2 and as a result are very appropriate for use in high power equipment such as circuit breakers. Use of SF_6-CF_4 also eliminates the need for current down-rating of apparatus under short fault conditions that is necessary with SF_6-N_2 insulation. This Master of Science Thesis research work reviews some essential theory of the breakdown mechanism in gases and details some of the dielectric properties associated with electronegative molecules, in particular, the family of fluorocarbons. Results from experimental determination of breakdown characteristics for various mixtures of SF_6-CF_4 at practical engineering pressures are presented. Data for 60 Hz alternating and positive polarity direct voltages, as well as standard lightning and switching impulse voltages for uniform, quasi-uniform and highly non-uniform electrode configurations at various gap lengths are plotted and analyzed. Corona inception voltages are also included as part of the ac and dc testing.

Table of Contents

List of Figures

List of Tables

1. INTRODUCTION

For many years the dielectric properties of several binary gas mixtures with sulfurhexafluride (SF_6) as the main constituent have been investigated; the underlying purpose being to find optimal mixtures whose electrical insulation properties exceed those of SF_6 alone. The constituent that is mixed with SF_6 can be a *buffer gas* (slows down high energy electrons through collision) such as nitrogen (N_2) or an *electronegative gas* (captures free electrons through attachment and forms negative ions) such as those of the halogen family of elements (Group VII of the periodic table). Gases can sometimes be tailored analytically and the properties of the resulting mixtures known before any experimental testing is performed. However, many mixtures display a "synergistic" effect where the overall breakdown strength exceeds the summed strengths of the individual constituents. The well known breakdown strength profile of SF_6-N_2 is typical of a positive sysnergism (described later).

In recent years, mixtures of SF_6 with the electronegative gas tetrafluoromethane or carbontetrafluoride (CF_4) have been implemented in the design of circuit breakers and switchgear and have been considered for use in dry-type distribution transformers of low kilovolt (kV) rating. The SF_6-CF_4 mixtures have been observed to possess a strong arc extinguishing characteristic that is far superior to that of SF_6-N_2 and a condensation temperature comparable to that of liquid N_2. However, aside from these traits there is presently an overall lack of knowledge concerning the properties of SF_6-CF_4 mixtures and only a small amount of data available on its breakdown strengths. It was therefore considered appropriate to pursue an experimental study of these mixtures as a Master of Science Thesis Research Project, the results of which could be used as a basis for any work that may be undertaken in the future.

This thesis presents a brief theoretical review of SF_6 and some of its useful binary mixtures followed by an investigation into some of the dielectric properties of the fluorogases. Finally, experimental studies of the breakdown strength of SF_6-CF_4 mixtures are made under ac and dc voltage stresses as well as standard lightning and switching impulse voltages for uniform, quasi-uniform and highly non-uniform electrode geometries.

2. IMPORTANT PROPERTIES OF SF_6 AND OTHER DIELECTRICS

2.1 History of SF_6:

Sulphurhexafluoride (SF_6) was first discovered in 1900 when Moissan and Lebeau [1] reported the first syntheses of a hexafluoride derivative of sulphur. Little scientific interest existed for practical applications of SF_6 until about 1940 when Cooper [2] suggested it might have a beneficial use as a dielectric gas in electrical power equipment. Further investigations at the Massachusetts Institute of Technology showed SF_6 to be an exceptional gas for use in Van de Graaff generators which in turn led to a rapidly developing interest in SF_6 for use in electrical power equipment such as gas-insulated switchgear (GIS), dry transformers, cable technology and other special purpose machines. In the last four decades, SF_6 has been the subject of many detailed investigations due to its remarkably high dielectric strength and other physical properties that are conducive to its use in electrical apparatus.

2.2 Some Fundamental Properties of SF_6

The widespread use of SF_6 as a high voltage dielectric is based on its high dielectric withstand of $\approx$90 kV/cm•bar [3]. This high dielectric strength is the result of SF_6 being an *electronegative gas*, that is it tends to trap free electrons and form negative ions of SF_6^-. For breakdown to occur in a gas, the rate at which electrons are produced must exceed the rate at which they are removed, so that the electron density increases exponentially to form a conducting (ionizing) path. The source of electrons can be from the electrodes, microdischarges within a system caused by particles, cosmic or other natural radiation-induced ionization, or from the gas itself as a result of collision detachment of an electron from a molecule or negative ion. Whatever mechanism is involved, free electrons will be generated within the system although whether or not an electron causes breakdown is related to the rate of electron multiplication and absorption in the region where it occurs. Other gases such as nitrogen (N_2) do not attach electrons and are subsequently referred to as *buffer gases*. Still others such as oxygen (O_2) have weak electronegative properties, though both (N_2 and O_2) have breakdown strengths which are substantially lower than SF_6.

Given a suitable dielectric strength, several other physical properties are essential for a practical dielectric. One is an appropriate operating temperature range. The dielectric strength of a gas depends (to the first order) on its density or the number of molecules per unit volume. If a sealed chamber is filled to a given density, then by the Boyle and Mariote Gas Law [3]:

$$pV = C$$

where: p = pressure
V = volume
C = constant

the density will remain constant until a change in temperature causes the gas to liquify, at which point the density and the dielectric strength of the remaining gas will begin to drop. At a practical engineering pressure of 340 kPa, SF_6 can be used to about -40 °C before liquifaction (condensation) begins. At this pressure SF_6 has a breakdown strength of $\geq$ 300 kV/cm. At the high end of the temperature spectrum SF_6 remains extremely stable, however when heated in the presence of common metals such as steel and copper, decomposition may begin as low as 200 °C. The liquifaction temperature of SF_6 (molecular weight 146) is very similar to that of carbondioxide (CO_2, molecular weight 44)[4]. Most molecules with a molecular weight near that of SF_6 are liquids or even solids at room temperature ($\approx$20 °C); the reasons for SF_6 remaining a gas are the results of intimate bonding between the fluorine (F) and sulphur (S) atoms and the fact that the resulting molecular configuration is highly symmetric.

As a dielectric gas, SF_6 possesses many advantages in that it is non-combustible, non-flammable and highly stable[a]. It is also colourless, odourless, tasteless and non-toxic to humans although when SF_6 undergoes arcing in the presence of trace amounts of O_2, H_2O, etc., toxic gaseous by-products are formed. Also when arcing takes place between metallic electrodes such as aluminium and copper, fine powder solid arcing by-products are formed that when mixed with water will generate hydrofluoric acid. Its electrical breakdown strength is substantially higher than that of traditional gases such as air, nitrogen and carbon dioxide and it has a better heat

a. SF_6 remains highly stable unless subjected to decomposition, at which time adverse compounds can be formed which will eventually destroy almost any system.

transfer ability than air or nitrogen due to its low viscosity and greater density. This of course leads to a more efficient gas circulation than could otherwise be obtained from air or nitrogen. SF_6 is also characterized by a superior arc quenching ability which when used in electrical equipment eliminates fire hazards, allows for considerable reduction in size and greatly improves overall system reliability. Essentially two properties of SF_6 make it an ideal arc interrupting medium, the large amount of energy required to decompose SF_6 into a plasma and the high dielectric strength of SF_6 even after arcing. A power arc takes place in a plasma with a core temperature at the centre of the arc in the range of 20000 °C. In puffer type circuit breakers where SF_6 is blown into through the arc, the tight binding of F with S within the SF_6 molecule ensures that the arc must continuously decompose the gas stream, thus the arc must give up a considerable amount of energy to the process of maintaining the plasma. As soon as sufficient energy is not available to decompose the SF_6 (when the arc current decreases toward current zero), the arc starts to extinguish. Once the arc has extinguished the SF_6 recombines very rapidly, mostly back into SF_6 although other by-products are formed and the resulting mixture generally has a dielectric strength at least as good as that of pure SF_6. Thus SF_6 has excellent properties for cooling and extinguishing the arc as well as a dielectric strength that increases very rapidly after arc extinction to a level undiminished relative to that before arcing.

Despite its many important advantages, SF_6 also possesses several disadvantages. One major problem as previously mentioned is its decomposition under electrical discharges which form lower fluorides of sulphur including SOF_2, SO_2F, SF_4 and SOF_4. These products produced are toxic and corrosive to many insulating and conducting materials. Other problems include a high liquifaction at higher pressures which restricts the use of pure SF_6 apparatus to indoor applications or warmer geographic areas. It must be manufactured synthetically which results in a high cost compared to traditional gases and also its dielectric strength is very sensitive to field non-uniformity which translates to a breakdown strength governed by local field enhancement due to protrusions, surface roughness and the presence of conducting particles in a system. Conducting particles and surface roughness caused by machining or scratches are known to enhance the local field stress. As a result, the intrinsic breakdown field strength of SF_6 cannot be fully exploited in practical applications. For SF_6 pressures of engineering interest and normal levels of surface roughness, partial discharge (PD) inception and breakdown voltages are the

same. However, PD without breakdown can occur for protrusions above the normal surface roughness. Conducting particles are the most frequent type of imperfection in GIS. Long, thin (wire-like) particles can actually be lifted by the electric field and will occasionally touch an electrode surface.

2.3 Advantages of Binary Mixtures:

The several disadvantages associated with the use of pure SF_6 as a dielectric medium have spurred investigations into tailoring gas mixtures for the varied needs of the electric power industry. Since no known single gas has been observed to meet all of the multiple needs and operation conditions that exist in power apparatus, many mixtures have been studied with the objective of tailoring the dielectric for a specific application.

Binary gas mixtures can frequently be classified into one of the following combinations:

- electronegative gas and a non-electronegative (buffer) gas;
- two different electronegative gases.

The electronegative and buffer gas mixture often provides the desirable property of capturing free electrons while at the same time scattering electrons of higher energy levels. Figures 2.1 and 2.2 provide an illustrative example of typical scenario. The electronegative SF_6 molecule can become an SF_6^- ion only after it has attached itself to a free electron. However, the effective attachment cross-section of SF_6 is such that only electrons in the low energy range of 0.0 to 0.2 eV may be captured (see Section 2.4). A buffer gas has no electronegative properties but rather slows down higher energy electrons by collision. Thus, addition of a buffer gas to a concentration of SF_6 more effectively slows down high energy electrons and brings them into an energy range where they may be captured via electron attachment. Some proven buffer gases used in SF_6-buffer mixtures include H_2, N_2, CO and CO_2; these mixtures manifest a significant positive synergism (the difference between the measured breakdown voltages of the mixture and the partial pressure weighted breakdown voltage of the component gases [5]). Alternatively, two different electronegative gases may be selected with each gas having its greatest electron affinity at different energy levels. For both types of binary gases, it is usually desirable to tailor the mixture such that as wide an energy range as possible to minimize the number of free electrons.

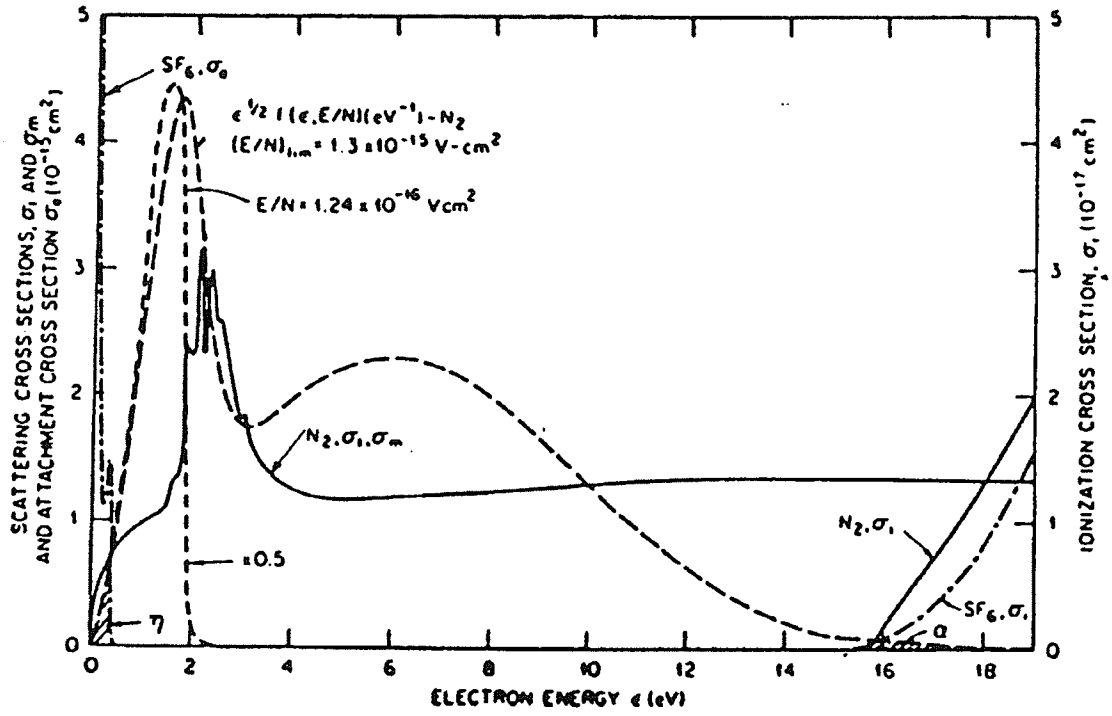

Figure 2.1
Ionization Cross-Section for SF_6 and N_2, Attachment Cross-Sections for SF_6

With knowledge of electron attachment, electron slowing down (buffering) and impact ionization of gases, one may choose and design a particular gaseous dielectric for some specific application. Probably the most effective means of preventing electrons from initiating a breakdown is to remove them by electron attachment so that the gas molecules may form stable negative ions. Inspection of Figure 2.2 shows that SF_6, although it is an electronegative gas, can only capture electrons of low energies since its electron attachment cross-section (see Appendix A) becomes small for electron energies above 0.4 eV. Thus high energy electrons associated with the enhanced field at a rough surface or at a particle will likely escape capture and initiate a breakdown. Although electron attachment cross-sections for other electronegative gases have been found to be higher than 0.4 eV, this becomes insignificant when the electron energies are above 1.2 eV. Thus for a good gaseous dielectric, not only must the electron attachment cross-section be as large as possible over as wide a range as possible, but the ability to reduce electron energies must be evident.

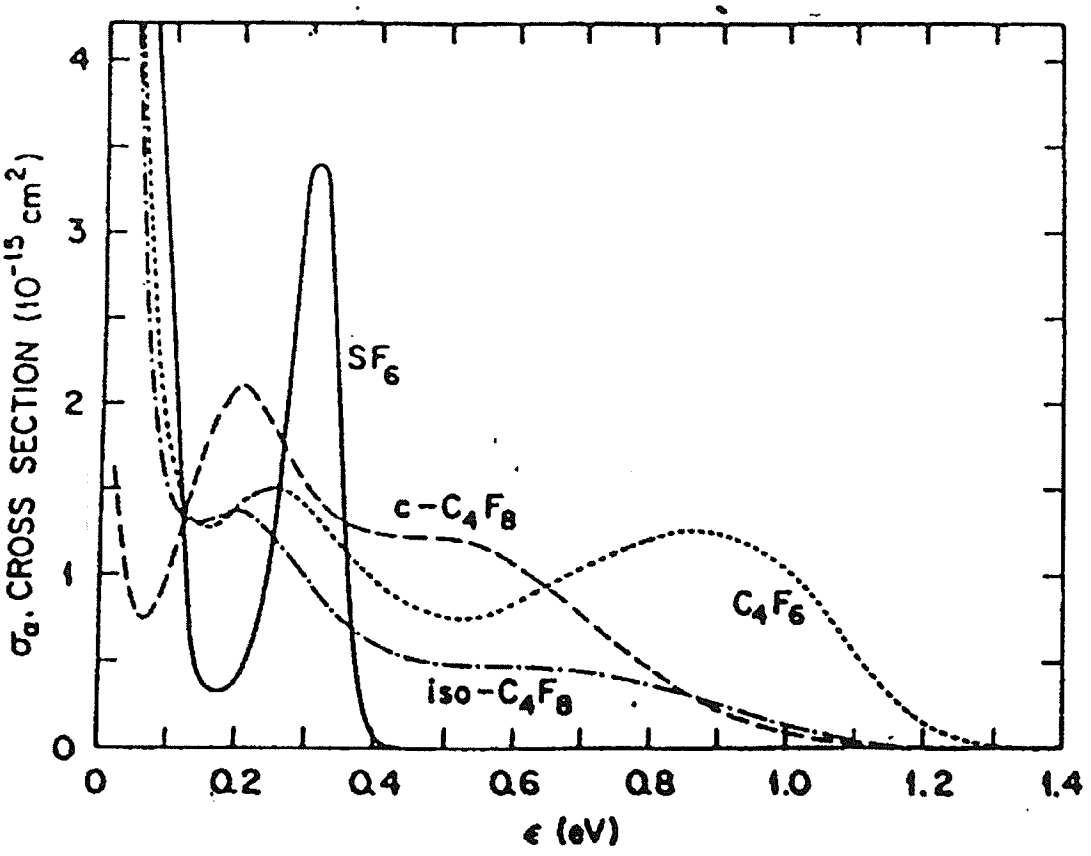

Figure 2.2
Attachment Cross-Section for SF_6 and Various Fluorocarbons

SF_6-N_2 mixtures are widely used due to N_2's good buffering ability[a]. A 50%SF_6-50%N_2 mixture at 15% higher total pressure than pure SF_6 exhibits the same dielectric strength at about 35% lower cost [6]. The SF_6-N_2 mixtures also have many other advantages over pure SF_6 such as a lower liquifaction temperature and a lower sensitivity to non-uniform fields and particle effects.

2.4 A Review of the Breakdown Mechanism:

As was mentioned in Section 2.3, the choice of a gaseous dielectric for a particular application should be based on the knowledge of electron attachment, electron slowing down and

a. N_2 possesses a strong negative ion resonance at about 2.3 eV which is very effective at slowing down electrons in this energy range.

electron impact ionization properties. Figure 2.1 shows that for a particular gas, given number density N under an applied electric field E, the free electrons attain an equilibrium energy distribution $f(\varepsilon,E/N)$ which is a function of the gas and E/N [7]. When the value of E/N is low ($\approx 1.24 \times 10^{-16}$ V•cm^2 for N_2), $f(\varepsilon,E/N)$ lies at lower energies and the number of electrons capable of ionizing the gas is negligible. However, as the voltage is increased, $f(\varepsilon,E/N)$ shifts to higher energies ε and for sufficiently high E/N the number of electrons capable of ionizing the gas is such that the gas makes the transition from insulator to conductor.

Figure 2.1 shows $f(\varepsilon,E/N)$ for N_2 and the limiting value of E/N ($(E/N)_{lim} \approx 13.00 \times 10^{-16}$ V•cm^2). Even at this high E/N value only a small fraction of electrons possess sufficient energy to induce ionization. This is denoted in Figure 2.1 by the shaded area a which is a measure of the ionization coefficient α/N which can be mathematically expressed as:

$$\frac{\alpha}{N} = \left(\frac{2}{m_e \cdot V_{drift}^2}\right)^{\frac{1}{2}} \int_{I_o}^{\infty} \underbrace{f\left(\varepsilon, \frac{E}{N}\right)\varepsilon^{\frac{1}{2}}\sigma_i(\varepsilon)\, d\varepsilon}$$

where: I_o = ionization threshold energy

m_e = rest mass of electron ($\approx 9.107 \times 10^{-31}$ kg)

V_{drift} = electron drift velocity

ε = electron energy

$\sigma_i(\varepsilon)$ = electron impact ionization cross-section.

The shaded area in Figure II.2 denoted by n is a measure of the effective electron attachment coefficient n/N_a expressed mathematically as:

$$\frac{\eta}{N_a} = \left(\frac{2}{m_e \cdot V_{drift}^2}\right)^{\frac{1}{2}} \int_{0}^{\infty} \underbrace{f\left(\varepsilon, \frac{E}{N_a}\right)\varepsilon^{\frac{1}{2}}\sigma_a(\varepsilon)\, d\varepsilon}$$

where: N_a = attaching gas number density

$\sigma_a(\varepsilon)$ = electron impact attachment cross-section.

Knowledge of α/N and η/N_a enables one to predict $(E/N)_{lim}$, which for uniform fields is defined as the value of E/N at which $\alpha = \eta$ (Note: $N = N_a$ for unitary electronegative gas).

3. INVESTIGATION INTO SF_6-CF_4 MIXTURES

3.1 Practical Implications:

In recent years, a large portion of the electric power industry has followed the international trend towards the use of single pressure SF_6 circuit breakers and gas insulated switchgear (GIS) for high voltage applications where good dielectric strength is essential (see Appendix B for GIS model). In many applications, switches (often referred to as disconnectors) are necessary to isolate components such as circuit breakers. In GIS, these disconnectors are used to isolate a breaker from the power system after the breaker has been opened. Normally two disconnectors are associated with each breaker, one on each side. Breakers with multiple interrupters have grading capacitors across the interrupters to assure equal voltage sharing during interruption (see Figure 3.1 for a typical power system GIS). Thus the first disconnector to be opened may have less than the full system voltage across it, unless the voltage on the two sides go out of phase upon opening the breaker as can happen when a generator is removed from a power system. The second disconnector to be opened will then see a floating (capacitive) load on one side and the system on the other. Under these circumstances, the floating side will follow the system side in a stepwise manner until the contacts of the disconnector have separated sufficiently to cause clearing [8]. At each step, a breakdown across the disconnector contacts equalizes the potential on the two sides of the disconnector, after which the potential on the floating side remains constant while that on the system side changes until the difference is again sufficient to cause a breakdown.

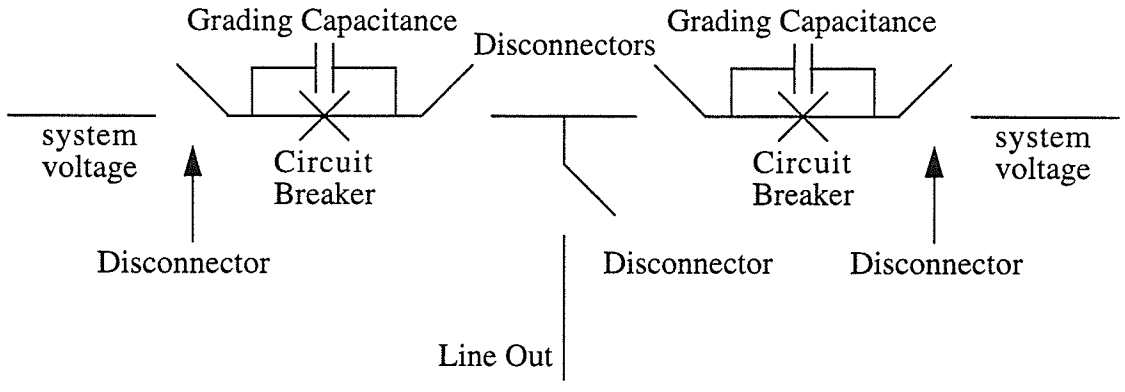

Figure 3.1
Typical Circuit Configuration for a Gas Insulated Substation

Analysis of these breakdowns within the disconnector reveals inhomogeneous field (leader or streamer) breakdowns between the electrodes. Just before such a breakdown occurs, the field is predominantly between the disconnector electrodes. However, once the leader has completed the path between the electrodes, they become approximately equipotential with respect to eachother and the field is predominantly from the electrodes and leader to the enclosure (ground). Now if upon completion of the leader between the contacts, the field from a leader branch to ground is sufficient to cause leader propagation to ground, then a ground fault will occur [8]. The probability of such a ground fault depends on the field configuration within the disconnector which is strongly affected by the maximum contact separation at clearing. This maximum separation is in turn affected by the design and statistical operating characteristics of the disconnector. In the worst case, clearing of the disconnector leaves a residual voltage (often referred to as trapped charge) of peak system voltage on the floating side of the disconnector. In this case, the disconnector contacts must be separated sufficiently to withstand peak-to-peak system voltage (else another intercontact breakdown will occur which means that the disconnector has not yet cleared). In the best case, the trapped charge will be near zero and the contact separation at clearing will only have to withstand a little more than peak system voltage. Thus the contact separation at clearing can vary by a factor of 2 depending on the design of the disconnector. This will of course have implications for the magnitude of switching transients, disconnector reliability, etc. and the statistics of trapped charge will therefore become important to disconnector design and operation. The trapped charge in turn depends on the difference between the withstand of the switch contacts for opposite polarities [9,10]. Switch characteristics are generally not symmetric with polarity because the electric field configuration around the switch contacts differs for the male and female contacts. This means that the field is more inhomogeneous on one side than the other, a basic asymmetry given that the source of free electrons and the breakdown process differ somewhat depending on whether the breakdown progresses from positive to negative electrode or the reverse.

Disconnector design becomes increasingly problematic with increasing system voltage. In circuit breakers, the number of interrupters is increased with system voltage and hence the voltage per interrupting stage can be kept fairly constant. However, disconnectors must be designed with only one interrupting gap for all voltages. With increasing voltage, the contact separation at

clearing increases which results in increased exposure of the periodic intercontact leaders to ground. To a large degree, the extensive investigations of inhomogeneous field breakdown in SF_6 were motivated by the need to design reliable disconnectors of ever higher voltage. With the improved understanding that has resulted from such studies, many aspects of disconnector and other component design and evaluation (for instance sensitivity to defects) can now be undertaken analytically, which has the important beneficial implications for system design and reliability.

Unfortunately, when SF_6 is becomes pressurized its condensation or liquifaction temperature greatly increases ($\approx$-30 °C @ 400 kPa) which makes it impractical for use in switchgear designed for outdoor operation in geographic areas where temperatures frequently plummet well below -30 °C. To overcome the liquifaction problems associated with pressurized SF_6, manufacturers often mix N_2 with SF_6. However, the thermal capability of SF_6-N_2 mixtures has been observed to be much lower than the thermal capability of pure SF_6 [11] which leads to a necessary current derating of electrical apparatus under short line fault conditions.

In attempt to overcome the reduction in thermal capability of SF_6-N_2 gas mixtures and to maintain a full interrupting rating of equipment should fault conditions arise, one possible option might be to compensate for the SF_6-N_2 mixture's reduced thermal capability by the inclusion of more grading capacity across the apparatus (circuit breaker or disconnector as was previously outlined) as well as shunt capacity connected at the line side. Unfortunately, choosing too high a value of grading capacity posses an increased risk of ferroresonance conditions. There is also a large expense involved with the addition of shunt capacity which may not be economically feasible. Thus, a second possible option might be to select or tailor a gaseous dielectric that maintains the thermal capability of pure SF_6 while at the same time retaining the low liquifaction characteristic of SF_6-N_2. At least one manufacturer has discovered that a mixture of SF_6-CF_4 satisfies these criteria at a fraction of the cost of implementing the first option.

SF_6-CF_4 gas mixtures were introduced as a dielectric medium in electrical apparatus to satisfy the same low-temperature purposes as the SF_6-N_2 mixtures; they even offer better arc quenching properties which make them appropriate for use in circuit breaker technology. Several preliminary investigations carried out by manufacturers and utilities have determined that the

SF_6-CF_4 mixtures have some practical advantages over SF_6-N_2, though there is still a great deal that is not known about these mixtures. For example, how does the dielectric strength of SF_6-CF_4 vary for various mixture proportions? How does the breakdown strength vary for different types of voltage stresses and for different field gaps? These are some typical questions that this thesis research attempts to answer experimentally. In lieu of an extensive analytical study into the dielectric characteristic of SF_6-CF_4, it seems more practical and expedient to limit the investigation to one based on experimental observation; the results of which can be further investigated at some future time if so desired. The preceding chapter was included to provide the reader with a basic understanding of the mechanisms involved with ionization and attachment in gases and how dielectrics may be selected or tailored to suit a specific application. An exhaustive amount of research into dielectric physics and the breakdown mechanism has been conducted within the last century and can be found in the literature. The purpose of this research is to investigate some physical properties of a gaseous dielectric that has proved useful in the design of efficient and cost effective switchgear. Emphasis is placed on trends found in the experimental data and how these trends can reflect real-world scenarios.

3.2 Some Physical Properties of CF_4 and the Fluorocarbon Family:

Gaseous fluorocarbons have long been of interest in high voltage applications because of their generally inert character and high dielectric strength. Fluorine chemistry is rather unique in that fluorine (the most reactive element in the periodic table) attacks nearly all other substances with the peculiar result that many of the combinations are among the most inert substances. For example, when fluorine attacks sulphur, the product (SF_6) becomes chemically, thermally and electrically stable. Other fluorogases including the Freons and fluorocarbons also offer high dielectric strength, low temperature of condensation (liquifaction), chemical inertness, non-toxicity, non-flammability and good heat conduction.

Fluorocarbon gases manifest wide variations in dielectric strength, however all invariably show a breakdown voltage which is greater than that of air or N_2. Figures 3.2 and 3.3 based on work by Camilli et al. [12,13] show the dielectric strength of typical fluorocarbon gases as affected by pressure when tested under positive standard lightning impulse and 60 Hz ac voltages.

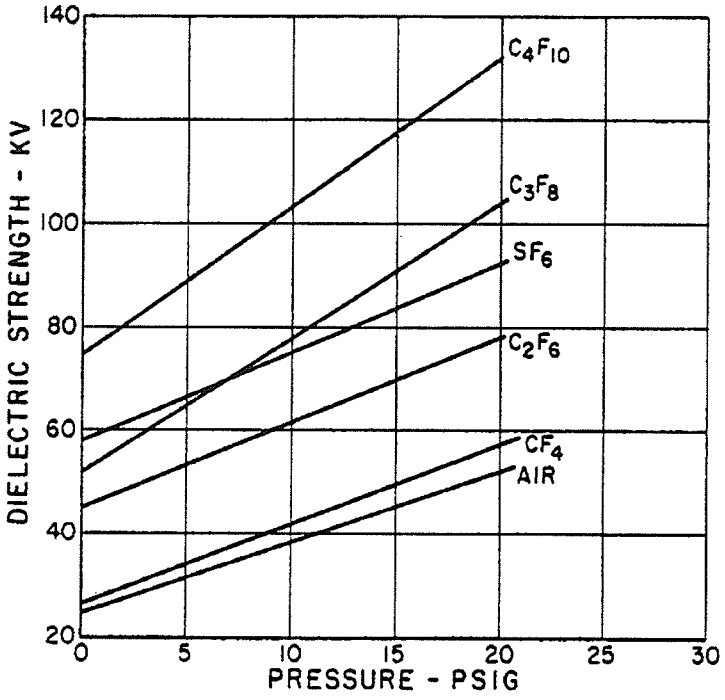

Figure 3.2
Positive Standard Lightning Impulse Breakdown Voltages (Rod-Sphere Electrodes, 25.5 mm Gap Length)

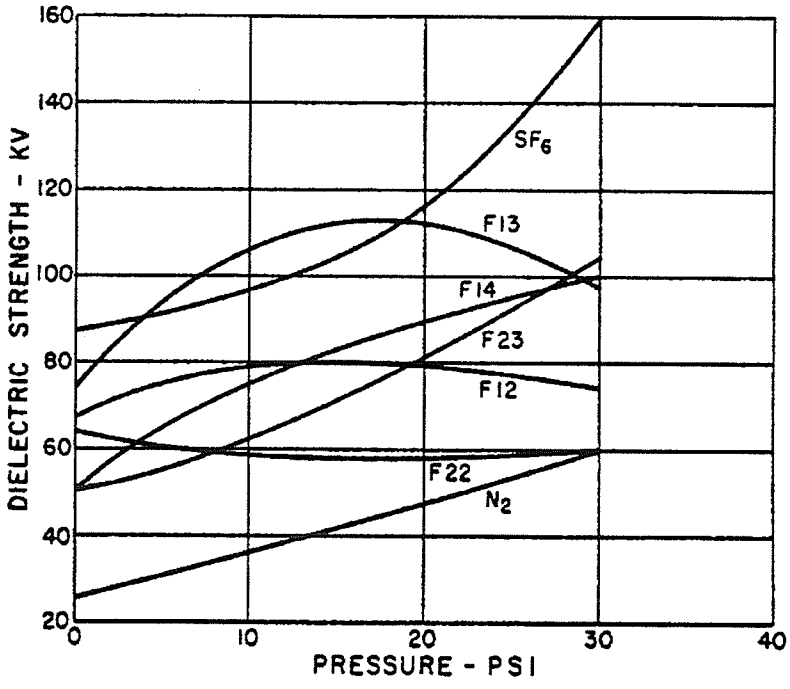

Figure 3.3
60 Hz ac Breakdown Voltages (Planar Electrodes of 76.2 mm², 12.75 mm Gap Length)

It can be seen from the standard lightning impulse tests in a highly non-uniform field that the dielectric strength of SF_6 remains substantially higher than that of CF_4 for all pressures tested (atmospheric to ≈200 kPa), but it is also seen that the breakdown voltages for CF_4 are at least 30 kV larger than those for N_2 for all pressures tested. Thus, even though CF_4 and N_2 (and air) are comparable under uniform field conditions, it is evident that the electronegativity of CF_4 comes into play when the field becomes divergent. Non-uniform fields are very difficult to analyze but at the same time are considerably important from a practical point of view. There have been several publications covering the breakdown in non-uniform fields [14,15,16]. It has been well established that under uniform fields, the breakdown voltages of fluorogases (including SF_6) increase linearly with increasing gas pressure as can be seen in Figure 3.3. However, in the case of non-uniform fields, Paschen's Law[a] [3] is generally not valid since the equation:

$$N_{cr} = e^{\int_0^l \bar{\alpha} dx}$$

where: N_{cr} = critical electron concentration giving rise to a streamer

$\bar{\alpha}$ = effective ionization constant

l = gap length (distance)

is not a function of the product *pressure•distance.* Breakdown voltages normally show an increase with gas pressure, but anomalies arising from space charge effects are sometimes observed.

An anomaly associated with the effect of pressure on non-uniform field gaps show that breakdown voltage increases with gas pressure to a maximum value at some pressure p_{max}. Above p_{max} there exists a regime of decreasing breakdown voltage with increasing pressure until a critical pressure p_{crit} is attained. At pressures above p_{crit} there is a slow increase of breakdown voltage with pressure [14,15]. This anomalous pressure effect has been observed only in electronegative gases and is not evident in non-attaching gases such as N_2 (see Figure 3.2). A possible explanation to this phenomenon is that streamer propagation across the gap is enhanced by reduced positive ion concentration and that photo-ionization may occur at higher pressures.

a. For a uniform electric field the breakdown voltage is a unique function of the product of pressure and the electrode separation for a particular gas and electrode material.

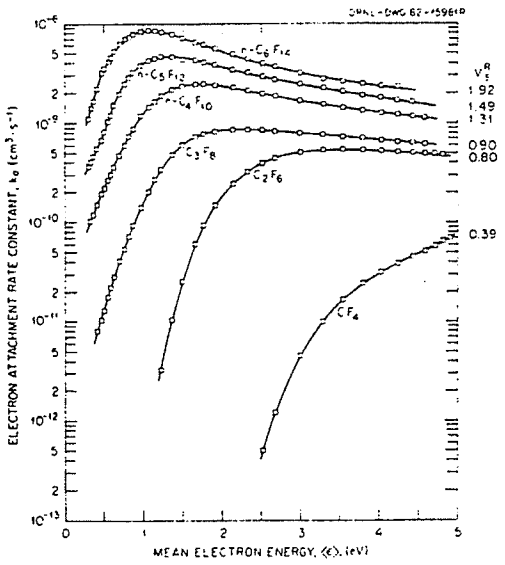

Figure 3.4
Typical Electron Attachment Rate Constants for Various Fluorocarbons

Figure 3.4 shows CF_4 to have good electron attachment properties for electron energies ≥ 2.5 eV and from Table 3.1 it can be seen that CF_4 has a much lower critical temperature[a] (-47.3 °C) and a much higher critical pressure[b] (≈3725 kPa) than all other fluorocarbons which are both very desirable properties for a gaseous dielectric.

Formula	Generic or Chemical Name	Relative Dielectric Strength	Boiling Point °C	Freezing Point °C	Critical Temp. °C	Critical Press. kPa
CF_4	Freon-14	1.3	-128.0	-184.0	-47.3	3723.2
C_2F_6	hexafluoro ethane	1.8	-78.0	-101.0	24.3	3288.8
C_3F_8	octafluoropropane	2.0	-37.0	-160.0	70.5	2675.2
C_4F_{10}	decafluorobutane	2.5	-2.5	-80.0	113.0	2013.3
C_5F_{12}	dodecafluoropentane	2.8	29.3	-125.5	na	na
SF_6	sulphurhexafluoride	2.0-2.5	-63.0	-50.8	54.0	3723.2

Table 3.1
Properties of Some Selected Fluorocarbons

a. That temperature above which a gas cannot be liquified by the application of pressure.
b. The minimum pressure under which a substance may exist as a gas in equilibrium with the liquid while being maintained at the critical temperature.

Ironically, the main disadvantage associated with the use of CF_4 as a dielectric is not science related but rather, bureaucracy related. Back in the mid-1950's when the Freon gases were considered ideal alternatives to ammonia for refrigerants due to their good chemical stability and low toxicity to humans, CF_4 was defined by government standards as Freon-14. Aside from being excellent refrigerants, the Freon family also manifested desirable electrical insulation properties and when used as dielectric gases, showed the expected electronegative characteristics of a typical halogen substituent. Freons are characterized by a high dielectric strength which in some instances has been cited to be equal to 8.5 times that of N_2 [4]. What was not known back in the mid 1950's however (and indeed not until the last decade), was that Freon gases have the ability to deteriorate ozone via chemical reaction. Subsequently, a significant depletion of the atmospheric ozone layer that protects the Earth's surface from the Sun's harmful ultraviolet spectral frequencies has prompted authorities to impose a global ban on the synthesis of all Freon gases by 1997.

Although the gas CF_4 has been generically labelled Freon-14, this is a misnomer as Freon gases typically contain atoms of carbon, fluorine and chlorine and are referred to as chlorinated fluorocarbons (coined "CFC's" by the non-scientific public). In reality CF_4 is the only Freon that does not contain the chlorine atom which is responsible for atmospheric ozone layer depletion. Obtaining a adequate supply of CF_4 to perform the research for this thesis was difficult to say the least. Just the mention of the word Freon invokes an apprehension which is not just isolated to the non-scientific community. The first bottle of CF_4 used to perform the preliminary work for this thesis was supplied from a manufacturer in Canada who at the time stated that no further CF_4 would be manufactured in this country due to its "environmentally adverse nature". When two additional bottles were required a few months later, the supplier had ceased distributing the gas due to government pressure for an all-out ban on Freons. As a result, the second and third bottles had to be ordered from the United States and did not arrive at the University of Manitoba for several months. It will be interesting to see if any additional supply CF_4 will be obtainable (at least in Canada) should any future research into this work be considered. Unfortunately, it is a government decision that CF_4 be banned from manufacturing and use by 1997 and unless any lobbying can be accomplished which classifies CF_4 as a non-Freon its use as a dielectric gas will likely be terminated.

4. EXPERIMENTAL APPARATUS

4.1 Circuits Used:

For the experimental studies of this thesis work, four high voltage circuits were employed to stress the SF_6-CF_4 dielectric mixtures:

- Positive Lightning Standard Impulse ($\approx 1.2 \times 50$ μsec)
- Positive Switching Standard Impulse ($\approx 250 \times 2500$ μsec)
- Positive Polarity Direct Current
- 60 Hz Alternating Current.

The circuit schematics and photographs of these setups are found in Figures 4.1-4.8.

Several different types of field gap were also employed to test the integrity of the dielectric mixtures under conditions which were considered to be representative of actual electrical apparatus. Each of the voltage stress types listed above (with the exception of dc) were applied to the following field configurations:

- Uniform Field Gap-

  Sphere-Sphere (ϕ62.5 mm) gap of 5 mm
- Quasi Uniform Field Gap-

  Rod (ϕ5 mm)-Sphere (ϕ62.5 mm) gap of 5 mm
- Highly Non Uniform Field Gap-

  Point (ϕ10 mm Rod tapered 30° to a tip of ϕ1.0 mm)-Sphere (ϕ62.5 mm) gap of variable length (0 mm to 30 mm).

Photographs of the uniform, quasi-uniform and highly non-uniform field gaps will be shown in Chapter 5 along with pictures showing detailed views of the point electrode prior to and after breakdown testing as seen by a scanning microscope at a magnification factor of 50. The "point" was effectively a spherical cap with radius of $\approx$ 0.5 mm.

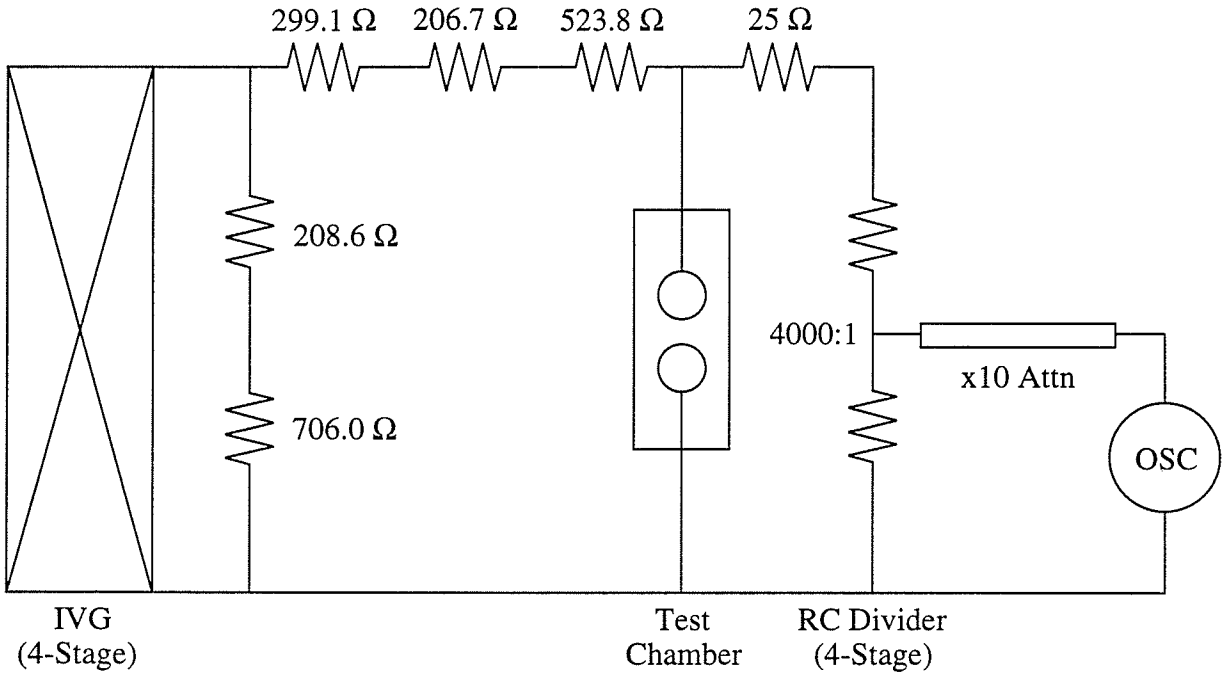

Figure 4.1
Circuit to Generate 1.2 × 50 μsec Standard Lightning Impulse Voltages (Positive Polarity)

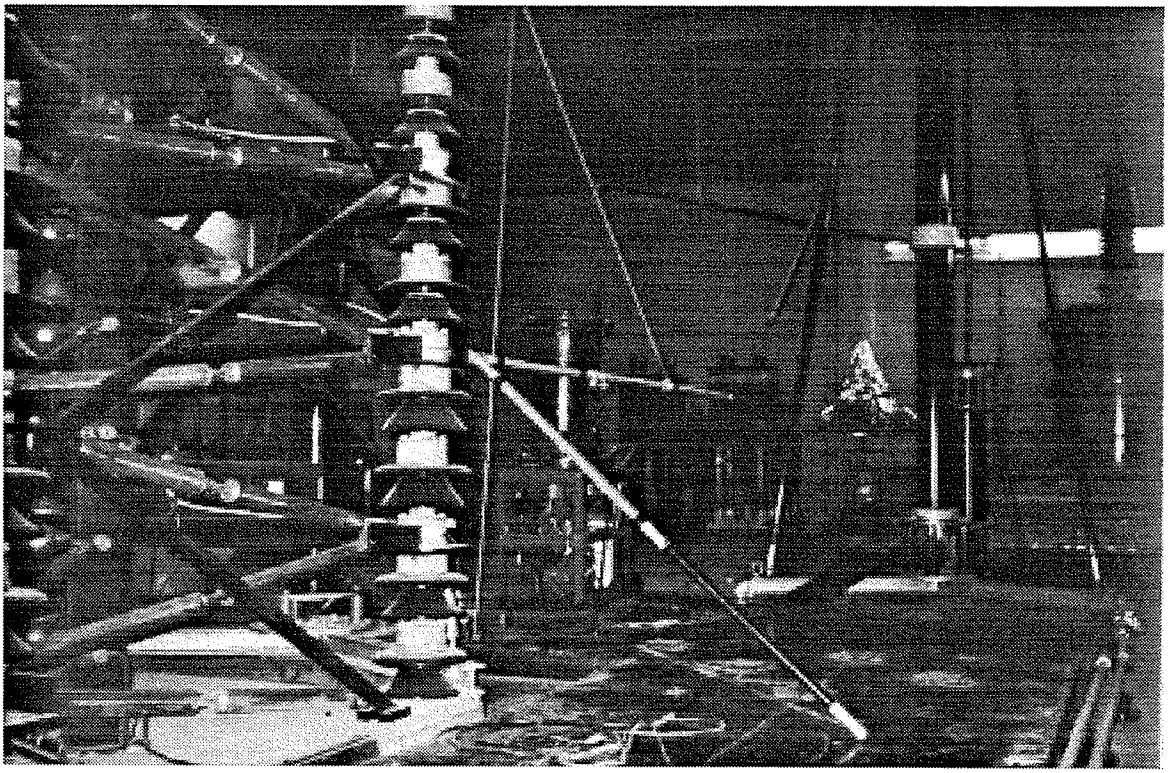

Figure 4.2
Photograph of Actual Circuit Shown in Figure 4.1

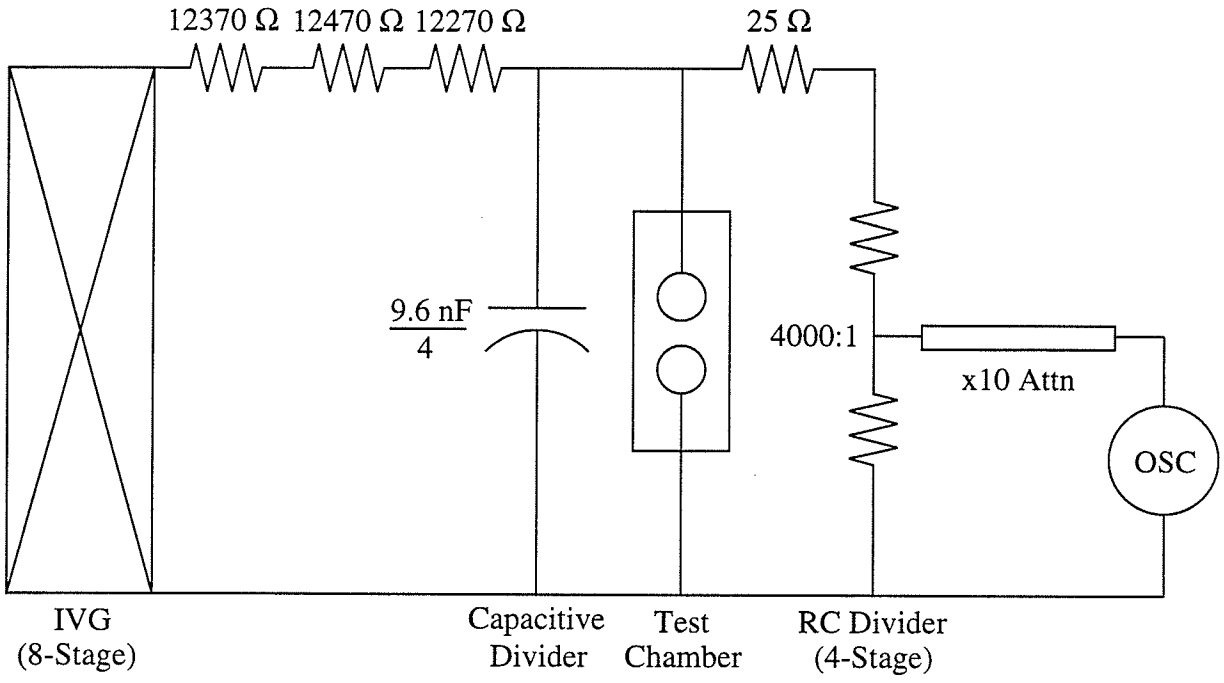

Figure 4.3
Circuit to Generate 250 × 2500 μsec Standard Switching Impulse Voltages (Positive Polarity)

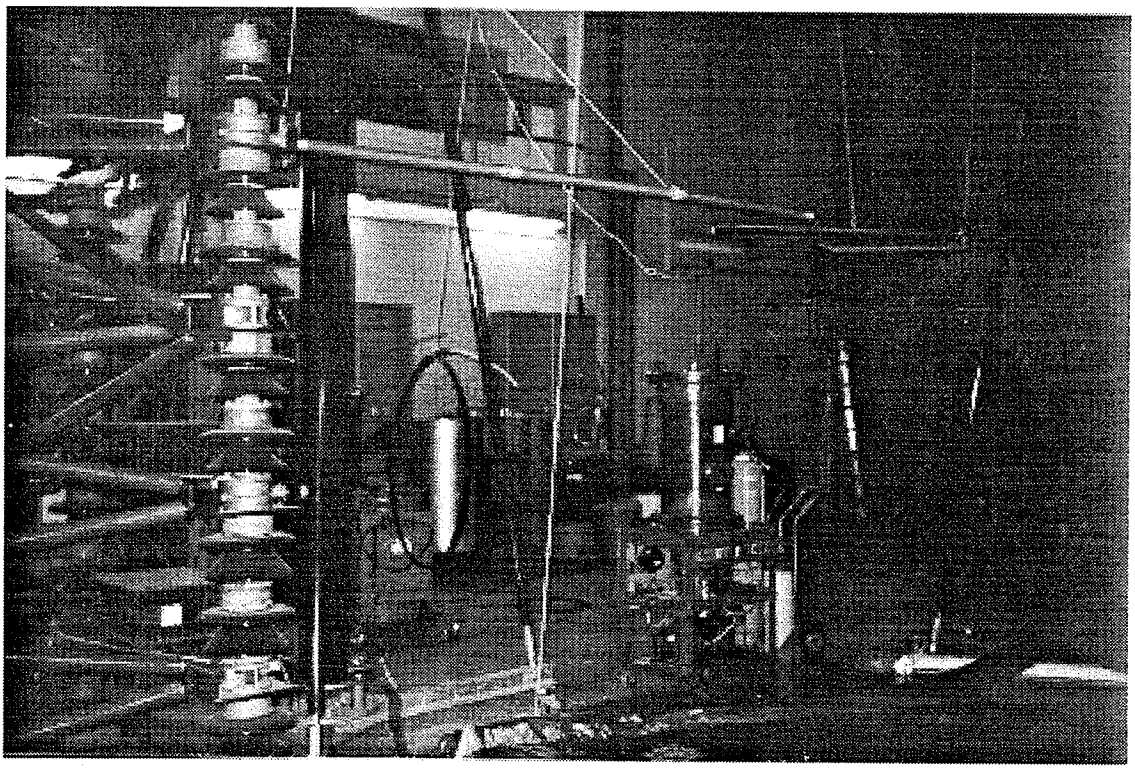

Figure 4.4
Photograph of Actual Circuit Shown in Figure 4.3

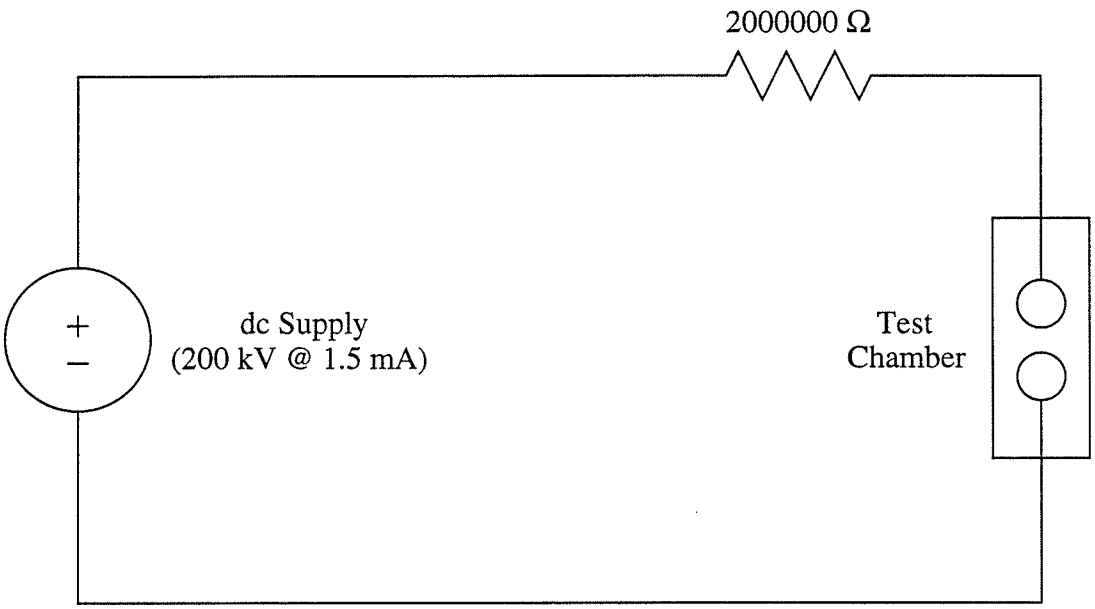

Figure 4.5
Circuit to Generate High Voltage dc

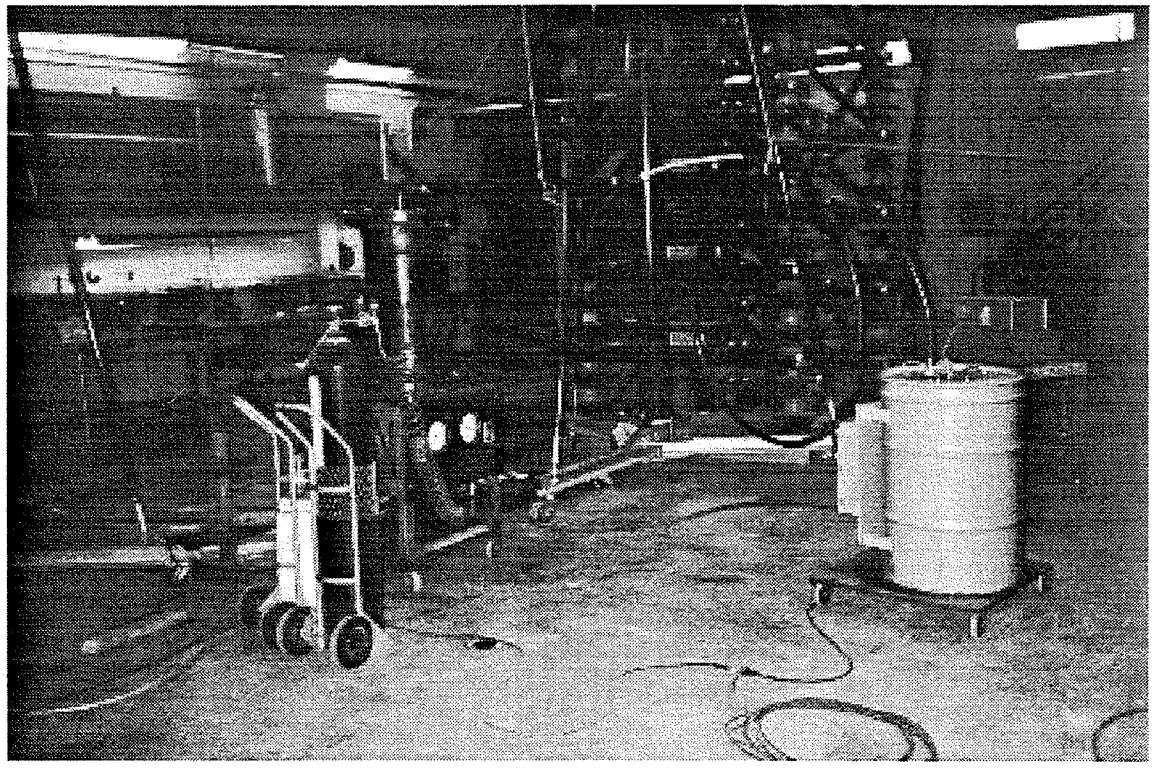

Figure 4.6
Photograph of Actual Circuit Shown in Figure 4.5

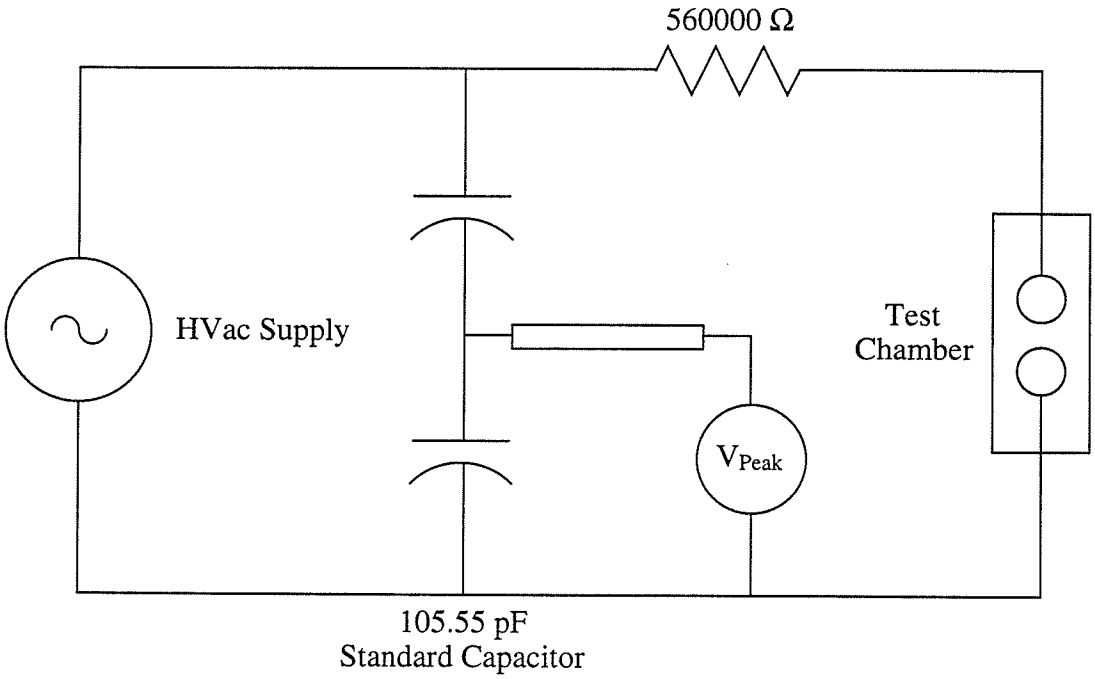

Figure 4.7
Circuit to Generate High Voltage ac

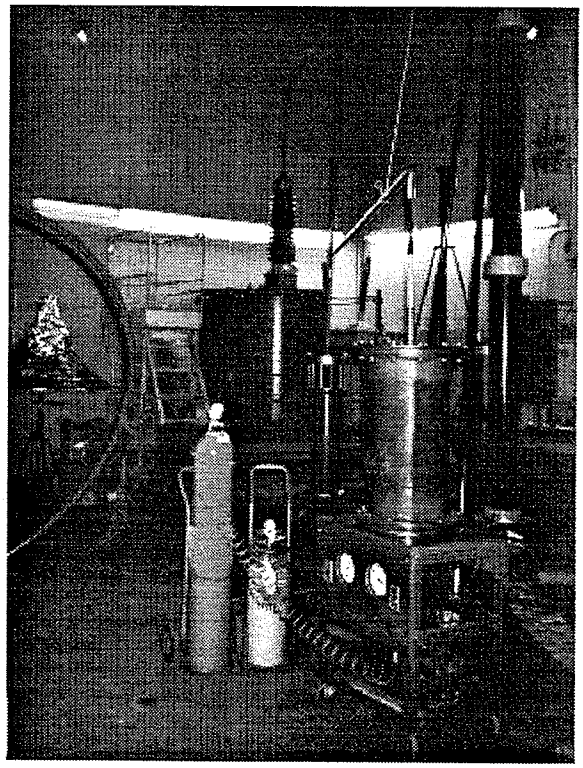

Figure 4.8
Photograph of Actual Circuit Shown in Figure 4.7

4.2 The Test Chamber:

The test chamber consisted of a fibreglass resin cylinder (ϕ350 mm $\times$ 825 mm) fitted with a brass plate (ϕ560 mm x 20 mm) at each end. The rated pressure of the vessel was specified as 700 kPa by the manufacturer. An acrylic frame was positioned inside the cylinder to support the electrodes (see Figure 4.9). A small dc motor geared to 3/4 rpm was used to rotate the bottom (earthed) electrode for gap adjustment. The shaft of the earthed electrode had a thread pitch such that one revolution corresponded to 1 mm linear motion. The shaft was also graduated so that measurements of gap length could be made with $\pm 15.0 \times 10^{-3}$ mm accuracy (see Figure 4.10).

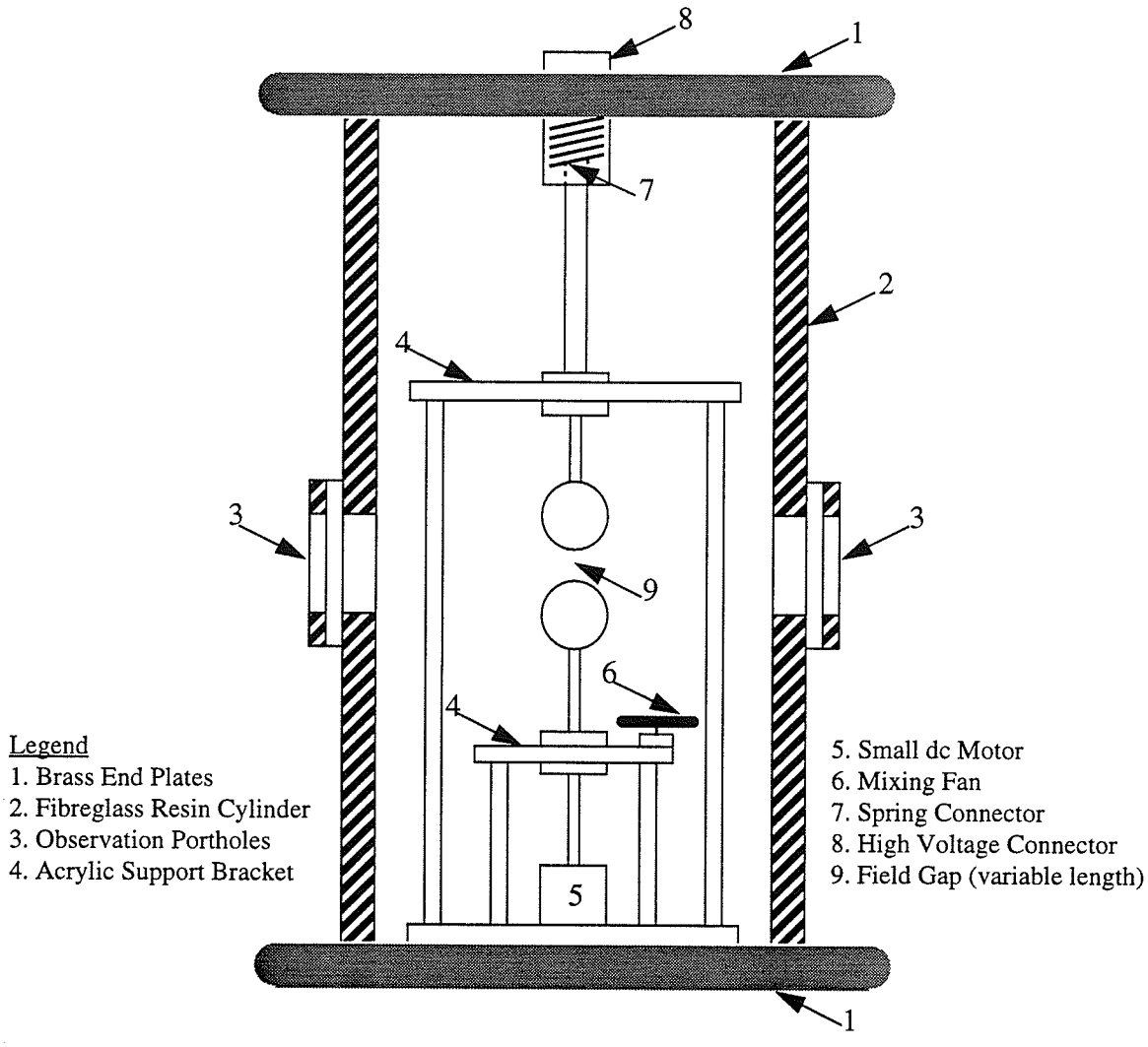

Figure 4.9
Cross-Sectional View of Test Chamber (Not to Scale)

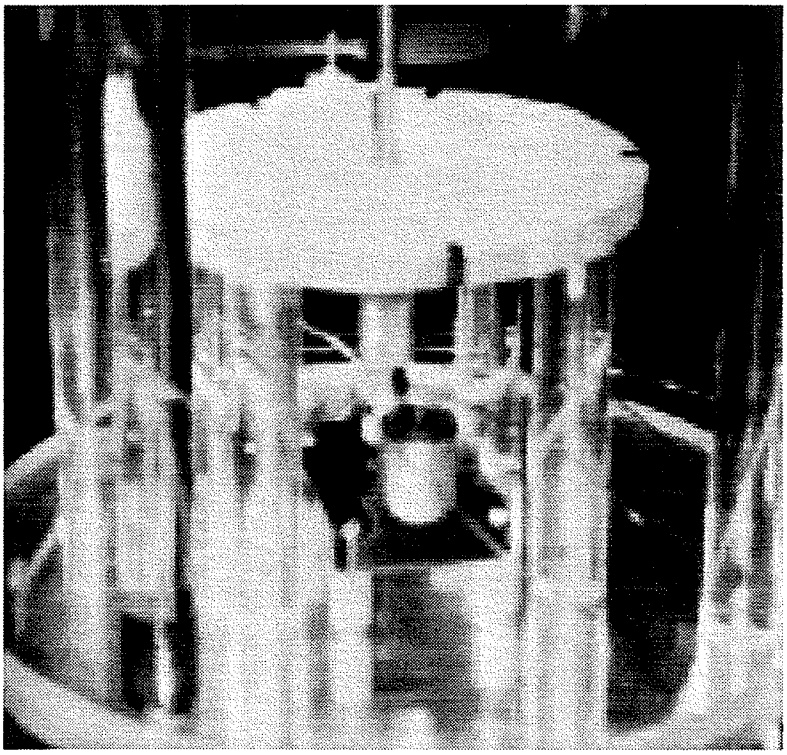

Figure 4.10
Detail View of Test Chamber Gap-Adjustment Mechanism

The direction of rotation of the gap adjustment mechanism was controlled by means of two double pole-double throw switches which could be operated from outside the chamber.

4.3 Gas Filling Procedure and Pressure Monitoring:

Prior to filling the test chamber with gas the vessel was evacuated to 0.0013 kPa (≈0.01 mm Hg), flushed with prepurified N_2 (99.995%) and then evacuated a second time to 0.0013 kPa. The test gas was then admitted into the chamber and the pressure was monitored by a Matheson pressure gauge (±0.25% error). Originally the gases were admitted into the chamber (see Appendix C for filling technique) and allowed to settle with no mixing. After the first phase of testing it was found that the breakdown voltages for SF_6-CF_4 mixtures under uniform field conditions were highly erratic (see Figure 4.11). Previous testing under similar conditions by others [11] have shown a linear relation for breakdown voltages of SF_6-CF_4 as a function of %SF_6 content per volume. These erratic data were believed to have been caused by two possibilities:

- When two or more dissimilar gases are allowed to settle in a closed vessel with no internal circulation they will form layers due their individual densities; this may lead to some breakdown instability at the layer interfaces.
- Over a period of a few days the pressure in the test chamber was found to drop by a fraction of a kiloPascal, thus if the gases inside the chamber were layered, then clearly they were not leaking out at the original mixing ratio; this also may lead to erratic breakdown voltage data.

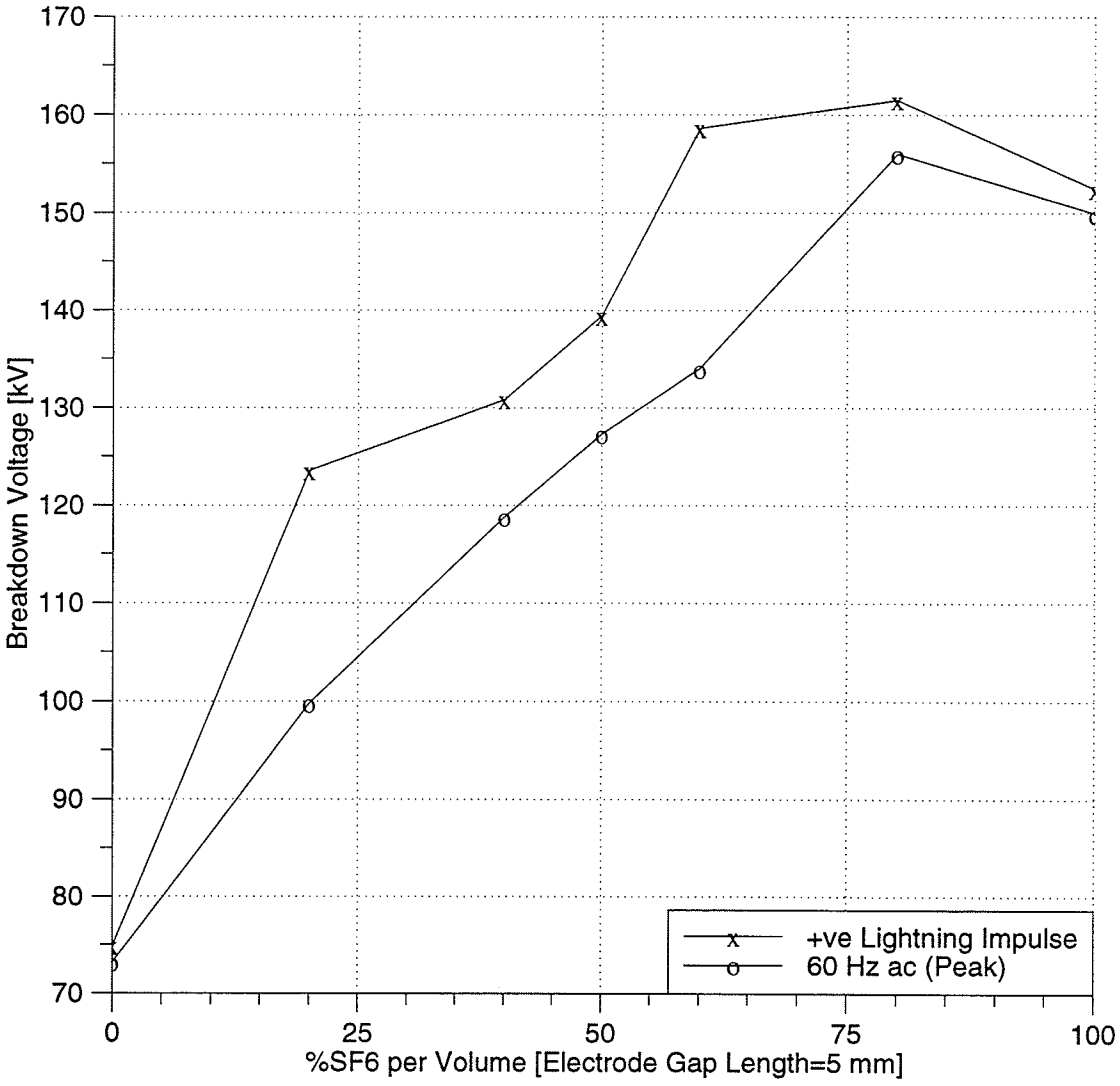

Figure 4.11
Sphere-Sphere (ϕ62.5 mm) Electrodes, 5 mm Field Gap, 300 kPa (before chamber refitting work)

In attempt to rectify these anomalies the chamber was completely dismantled and refitted with new parts. O-rings were custom manufactured and installed at the interface between the fibreglass resin cylinder and each brass endplate, existing copper pressure lines were replaced with new nylon lines where required, existing ferules and valves were replaced with new ones where necessary and a small mixing fan was fastened to the acrylic support frame to provide internal circulation for the gases. Finally, the complete pressure system was charged to 700 kPa and all connections and interfaces were thoroughly checked for leaks with a soap and water solution. A repeat of the test of Figure 4.11 showed good agreement with Reference 17 data (see Figure 4.12).

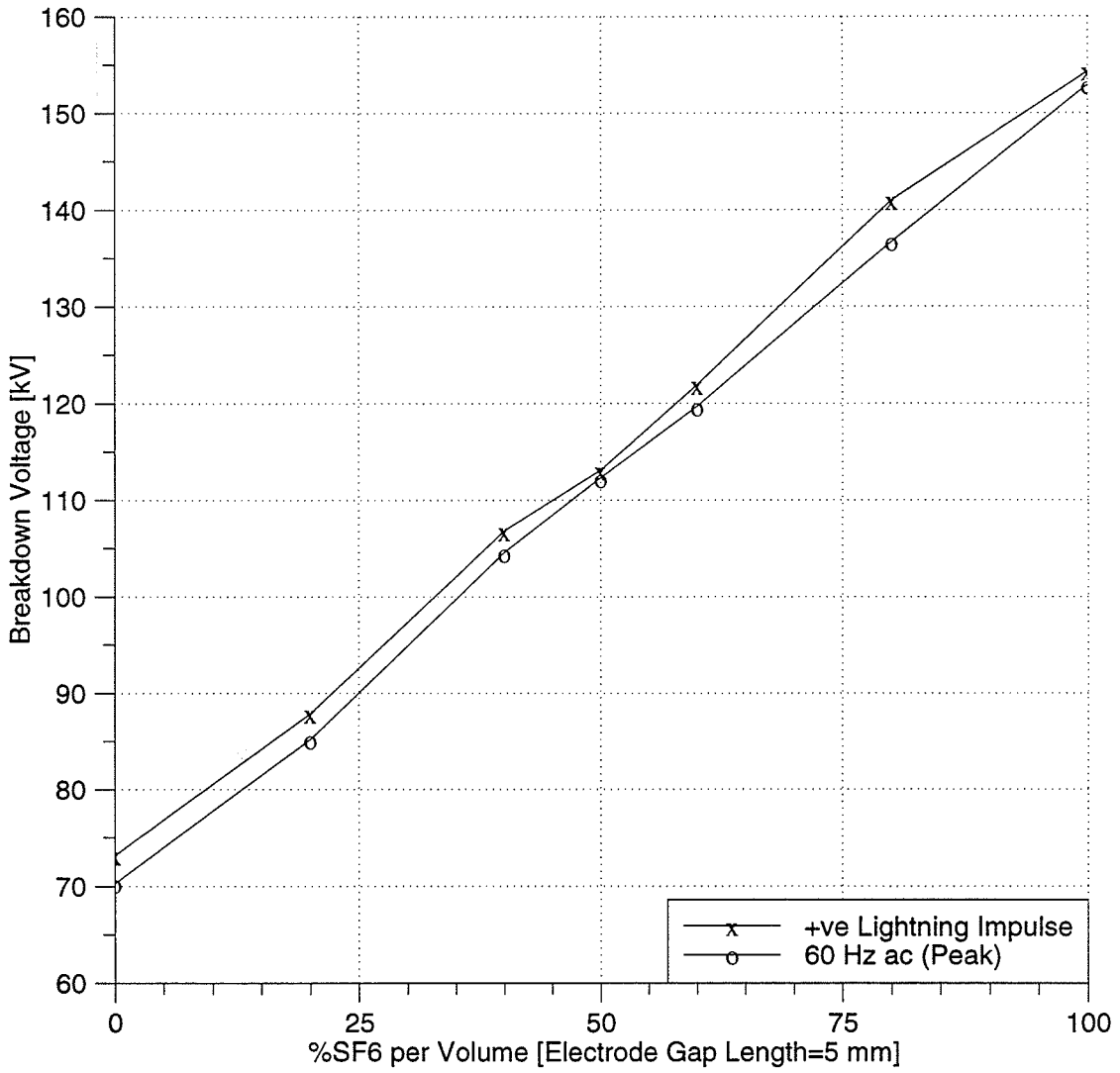

Figure 4.12
Sphere-Sphere (ϕ 62.5 mm) Electrodes, 5 mm Field Gap, 300 kPa (after chamber refitting work)

4.4 Test Procedures:

4.4.1 Standard Lightning Impulse Voltage Tests:

An approximate 1.2 × 50 μsec positive polarity impulse voltage was generated in accordance to IEC 60-1 Standards [18], the circuit of which is illustrated in Figure 4.1. The purpose of this test was to observe the effects of fast-fronted voltage stresses on the SF_6-CF_4 mixtures. For determination of the 50% breakdown voltage, the Up and Down Method [18] was used starting from a reference voltage stress and either going up or down 3% depending on whether a withstand or breakdown occurred. Due to the large amount of data generated from testing process, a computer program in *C* was written to calculate the 50% breakdown voltage and the standard deviation from a set of data (see Appendix D for program listing). For each test, no less than 15 shots were applied with a 1 minute waiting interval between each shot. Figures 4.13 and 4.14 show respectively the voltage magnitude as a function of front and tail times of the generated impulse. The wave front was calculated based on a rise of 30%-90% of the peak value.

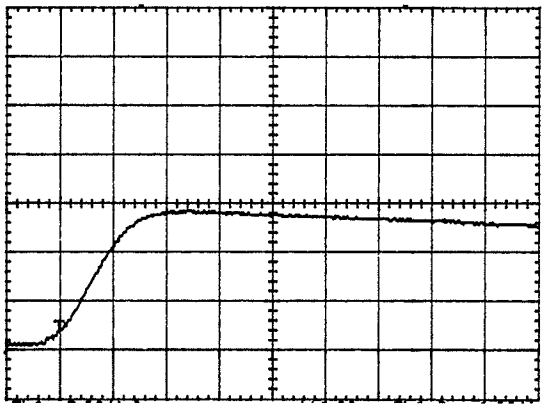

Figure 4.13
Standard Lightning Impulse Wave Front
(Time Scale = 1.0 μsec/div)

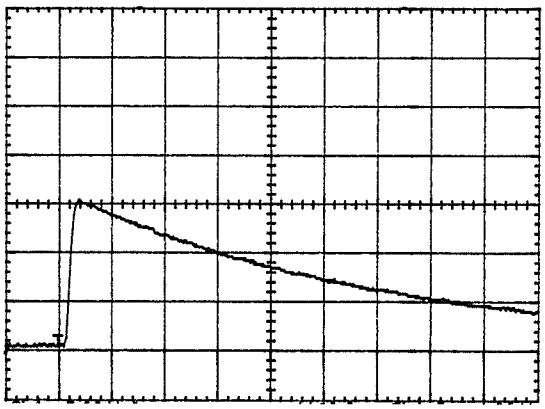

Figure 4.14
Standard Lightning Impulse Wave Tail
(Time Scale = 10.0 μsec/div)

4.4.2 Standard Switching Impulse Voltage Tests:

Since most electrical switchgear and circuit breakers are subject to a greater number of mechanical switching surges than actual lightning surges in their operational lifetimes it was considered feasible to study the effects of slow-fronted voltage stresses on the gas dielectric under test. In standard lightning voltage tests an insulation is subjected to a very large *dv/dt* value, whereas in standard switching voltage tests the insulation must be able to withstand a high voltage stress for a long period of time since *dv/dt* is much smaller; thus manufacturers and utilities may find the data from the latter to be of more practical relevance. To conduct this test an approximate 250 × 2500 μsec positive polarity impulse was generated in accordance to IEC 60-1 Standards [18], the circuit of which is shown in Figure 4.3. The Up and Down Method was again used to determine the 50% breakdown voltage and standard deviation of the test data. As with the standard lightning voltage investigations, no less than 15 shots were applied for each test with 1 minute waiting interval between each shot. Figures 4.15 and 4.16 show respectively the voltage magnitude as a function of front and tail times. The front of the generated impulse was calculated from the actual origin to the voltage peak.

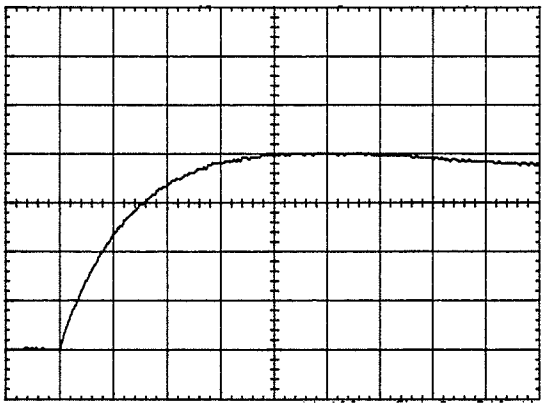

Figure 4.15
Standard Switching Impulse Wave Front
(Time Scale = 50 μsec/div)

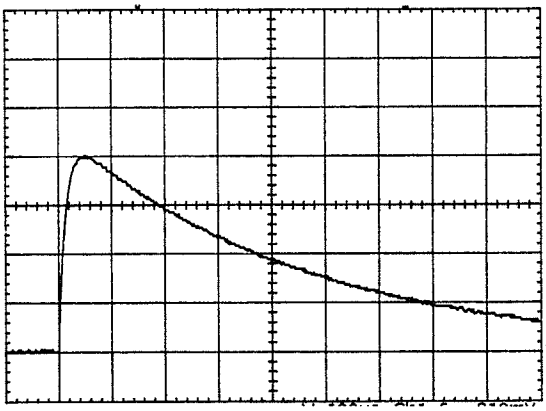

Figure 4.16
Standard Switching Impulse Wave Tail
(Time Scale = 500 μsec/div)

4.4.3 Positive Polarity dc and 60 Hz ac Voltage Tests:

To test the integrity of the SF_6-CF_4 mixtures under non-transient, steady state conditions, 60 Hz ac and positive polarity dc voltage stresses were applied to the gas mixtures until breakdown occurred. The testing procedure was carried out as specified in the IEC 60-1 Standards [18] and no less than 5 voltage applications were made for each test with a 1 minute waiting interval between each application. The arithmetic mean breakdown voltage was taken as the 50% breakdown voltage was determined as follows:

$$V_{50} = \sum_{i=1}^{k} \frac{(V_{BD})_i}{n}$$

where: V_{50} = 50% breakdown voltage

V_{BD} = breakdown voltage at application i

n = total number of applications.

The standard deviation of the data was then calculated using the following equation:

$$\sigma = \left(\sum_{i=1}^{k} \frac{((V_{BD})_i - V_{50})^2}{n^2} \right)^{\frac{1}{2}}$$

where: σ = standard deviation.

Finally, corrected values for pressure and temperature were calculated using the following:

$$V_{Corrected} = \left(\frac{Pressure\,[kPa]}{101.325\,[kPa]} \right) \cdot \left(\frac{295.15\,[K]}{Temperature\,[K]} \right) \cdot V_{50}.$$

Corona inception voltage was measured on a cathode ray oscilloscope across a current shunt resistor of 5 kΩ connected in the chamber ground. This technique worked well for higher voltages however for lower voltages (< 50 kV) and for pure SF_6 no observable corona could be measured on the oscilloscope. Protection was provided by a sphere gap in shunt with the 5 kΩ resistor.

5. RESULTS OF EXPERIMENTAL RESEARCH

5.1 Uniform Field Conditions:

As mentioned in Section 4.3, before refitting the chamber with new parts the data obtained for SF_6-CF_4 mixtures were very erratic. However, after the installation of a mixing fan inside the chamber and ensuring the vessel was well sealed from any leaks, the test data became much more stable and appeared to be in good agreement with previously obtained results by others. Figure 5.1 shows a view of uniform (Sphere-Sphere) electrode configuration for a fixed gap length.

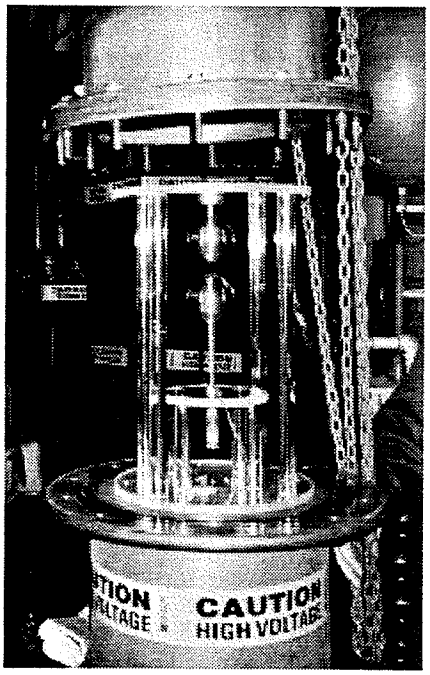

Figure 5.1
Photogragh of Uniform (Sphere-Sphere) Field Configuration at a Fixed Gap of 5 mm

This photo was taken at the onset of the experiment prior to the chamber refitting work (notice the gap length had to be manually set by rotating the lower sphere to the desired height). After setting the gap, the chamber cylinder was lowered over the electrode arrangement and sealed by tightening the chamber lug bolts. There was a considerable degree of error involved with this gap setting procedure due to the fact that once the chamber was sealed there was no means of monitoring the gap length other than a visual inspection through the observation portholes.

The data obtained with the positive lightning impulse and ac voltage breakdowns for a fixed Sphere-Sphere gap length of 5 mm as a function of $\%SF_6$ at 300 kPa pressure are shown again in Figure 5.2.

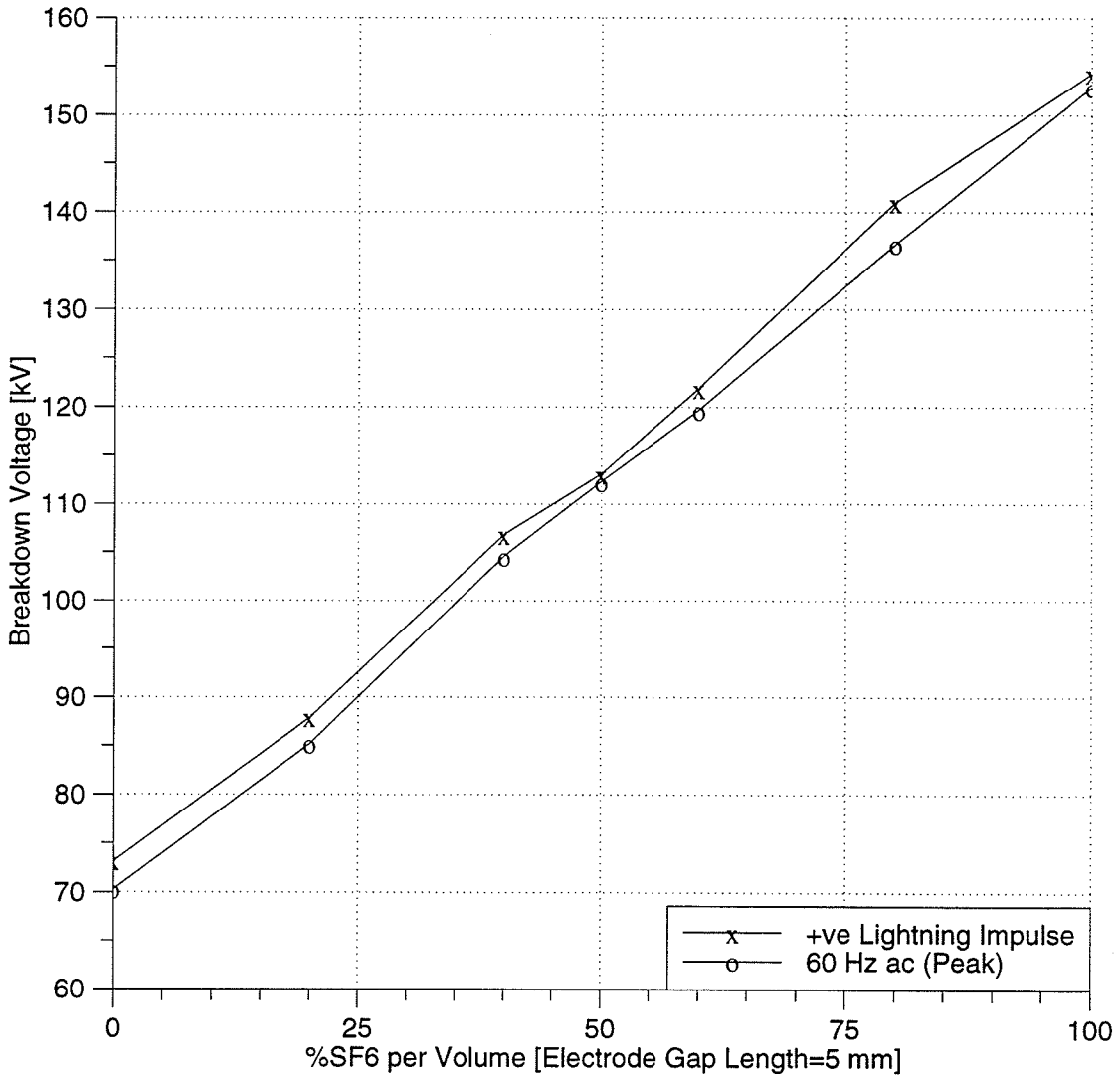

Figure 5.2
Breakdown Voltages of SF_6-CF_4 Mixtures (Sphere-Sphere (ϕ62.5 mm), 5 mm gap, 300 kPa pressure)

The magnitudes of the positive lightning impulse and ac are comparable with eachother; the positive impulse breakdowns are slightly higher than those for ac but are in good agreement with results obtained by others [11,17]. For the preliminary tests no dc source was available, though for uniform field gaps, breakdown under positive polarity dc should be similar to ac breakdown data.

5.2 Quasi-Uniform Field Conditions:

After the accuracy of the testing technique was established and the reproducibility of data proved, the test chamber was opened and the Sphere-Sphere electrode gap replaced with a Rod-Sphere gap (see Figure 5.3). The ϕ3 mm rod was hemispherically capped at one end and the gap length was fixed at 5 mm (this electrode configuration was assembled and tested under voltage stresses prior to the installation of the gap adjustment mechanism, although the gas mixing fan had already been installed).

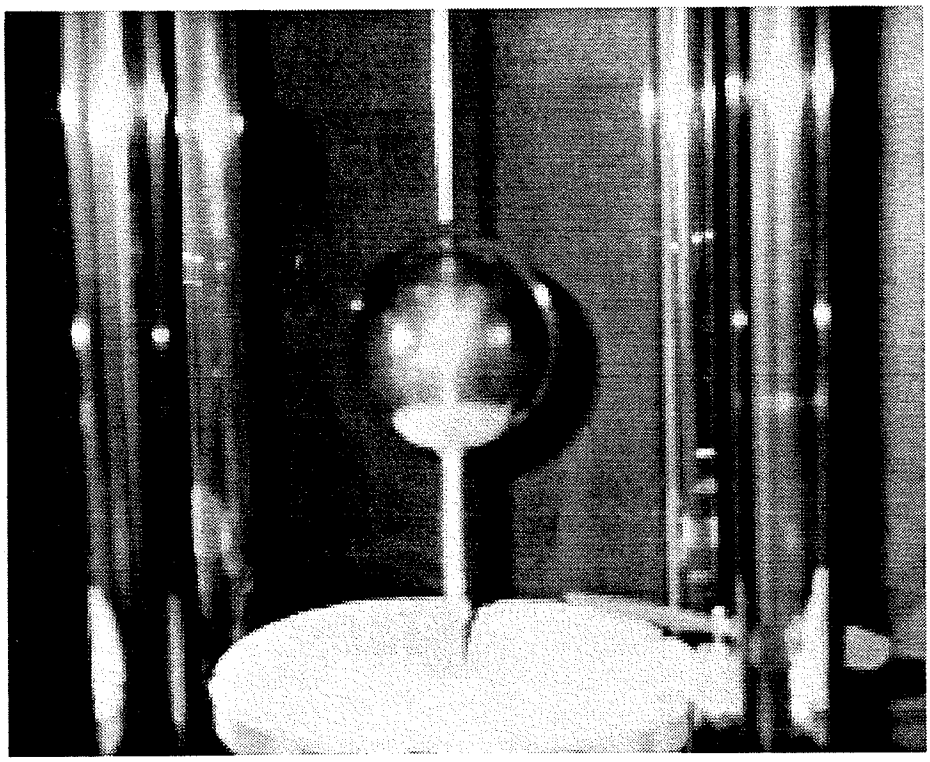

Figure 5.3
Photograph of Rod (ϕ3 mm)-Sphere (ϕ62.5 mm) geometry with field gap of 5 mm

The purpose for this choice of electrode configuration was to setup a non-uniform field condition, though with the small fixed gap length the field distribution turned out to be quasi-uniform as the breakdown voltage data of Figure 5.4 indicates. It may have been beneficial to scan images of the hemispherically capped rod prior to and after completion of the testing with a microscope for analysis and archival purposes; unfortunately this was not considered at the time.

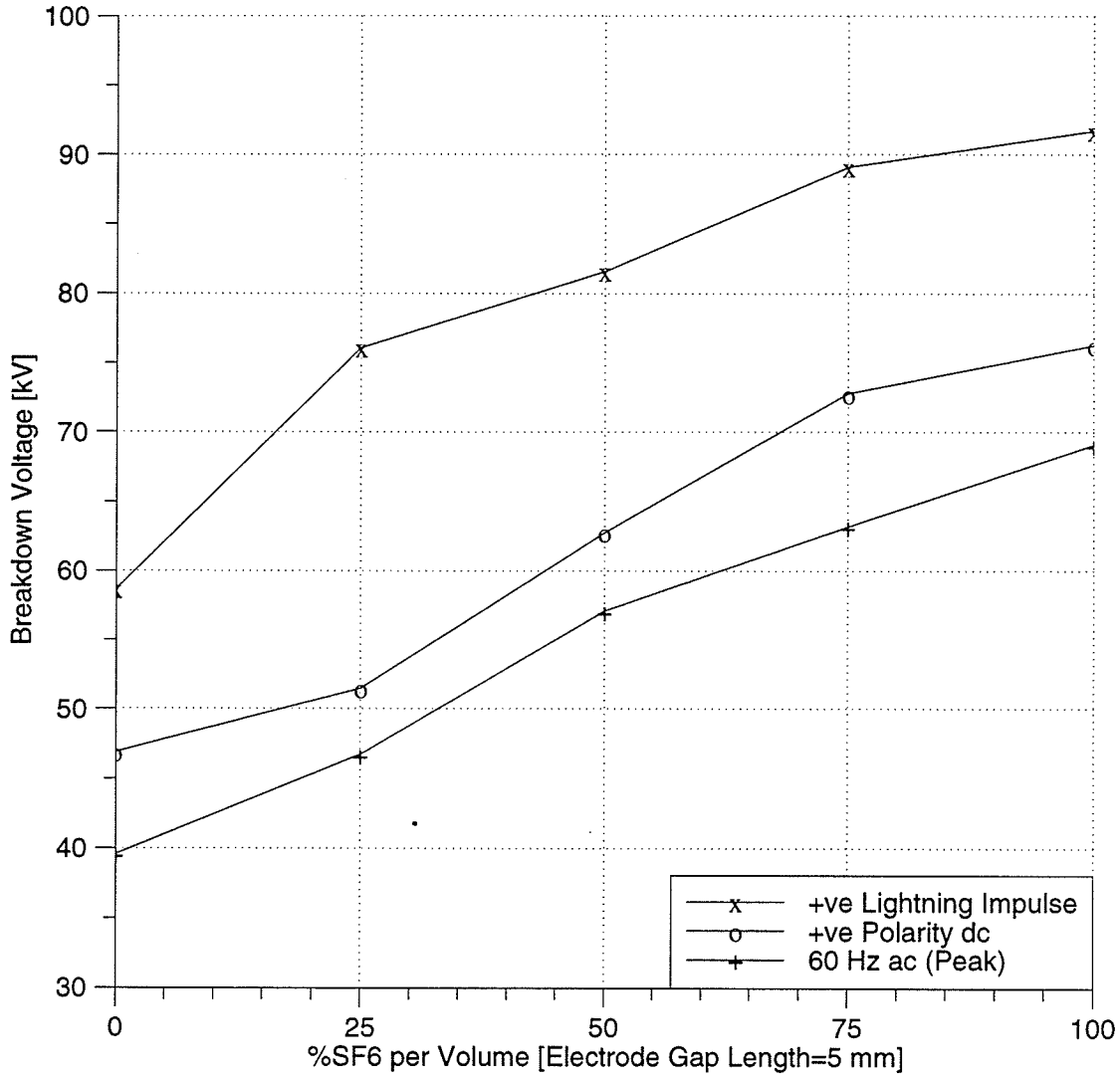

Figure 5.4
Breakdown Voltages of SF_6-CF_4 Mixtures under Quasi-Uniform Field, 300 kPa Pressure

Investigation of these data reveal some interesting trends. The overall linearity of the curves confirm a quasi-uniform field condition. However, unlike the uniform field data of Figure 5.2, the lightning impulse breakdown voltage magnitudes of Figure 5.4 are on average 15-25 kV higher than the ac magnitudes; this relation suggests a lack of sufficient time for the establishment of space charge. The SF_6-CF_4 mixtures also appear to have good dielectric properties for quasi-uniform field conditions, though the breakdown voltages are well below those obtained for the uniform field conditions. A comparison test with SF_6-N_2 mixtures showed the well-established synergism relation [19] which was further indication of a quasi-uniform field.

5.3 Highly Non-Uniform Field Conditions:

Until this point all testing had been conducted under fixed gap conditions. Due to the limited scope of observations that can be made for a single gap length and the high cost of CF_4 compared to other more common gases, it was considered beneficial to devise a gap-adjustment mechanism to extend the scope of observations to several gap lengths. The earthed electrode was fitted with an isolated dc motor geared to 3/4 rpm (see Figures 4.9 and 4.10 for views of the gap- adjustment mechanism), the shaft of which was threaded such that 1 revolution = 1 mm linear displacement. Both the gas mixing fan and the gap-adjustment motor were wired so that they could be independently controlled from outside the chamber; this eliminated the need to open the chamber for reasons other than changing electrodes. Figure 5.5 shows a picture of the Point-Sphere electrode configuration used for the non-uniform testing.

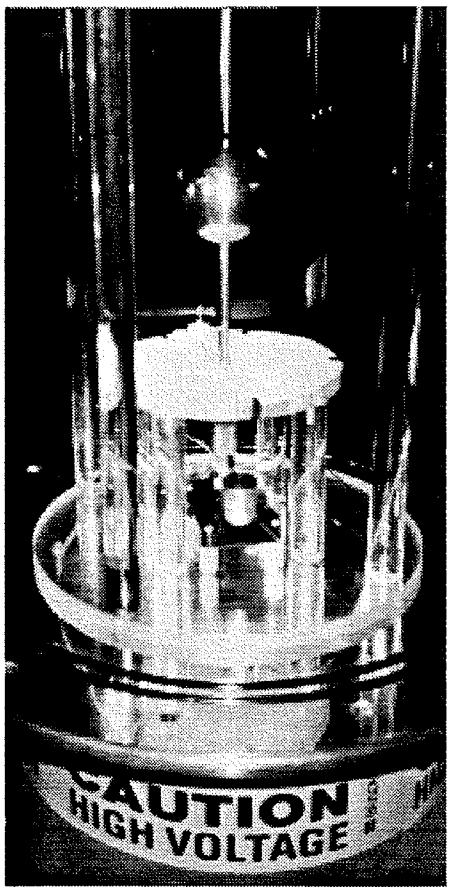

Figure 5.5
Photograph of Point (ϕ10 mm rod tapered by 30° to a tip of ϕ1.0 mm)-Sphere(ϕ62.5 mm) Geometry

Using the gap-adjustment mechanism, any gap length within the range of 0 to 30 mm could be accurately measured and maintained. Figure 5.5 also shows the acrylic support bracket and the vulcanized high vacuum O-rings. Prior to testing, both support bracket and inside of the chamber cylinder were thoroughly wiped down with methanol (proper choice of cleaning solvent is critical and care must be exercised not to use hydrocarbon (petroleum) based solvents such as Varsol that leave a film and could diminish the dielectric properties of the insulated materials). Before the chamber cylinder was lowered, a thin layer of high vacuum grease was applied to the O-rings to ensure a good seal once the chamber lug bolts were tightened.

Figures 5.6 and 5.7 show a ×50 magnification of the tip of the point electrode prior to and after completion of testing. The "point" electrode was fabricated from a ϕ10 mm rod. The rod was then conically tapered by machining to an angle of 30° and terminated by a tip of ≈0.5 mm radius[a].

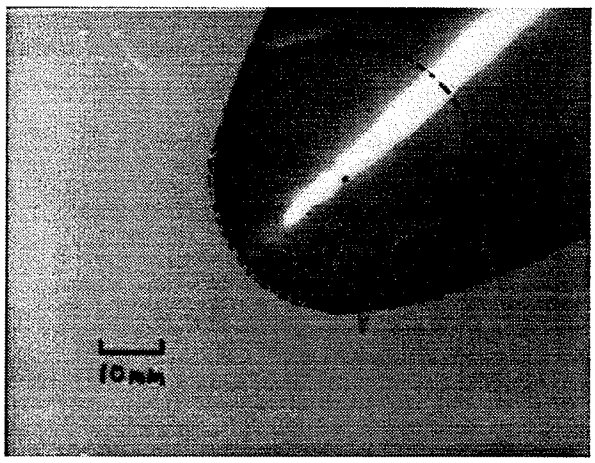

Figure 5.6
Profile of Point Electrode Prior to Testing
(Image at ×50 magnification)

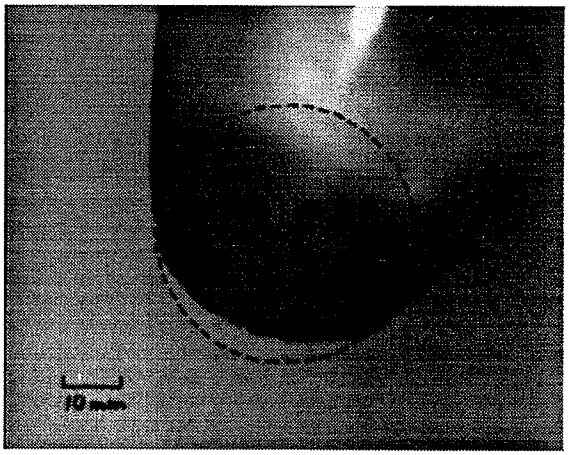

Figure 5.7
Profile of Point Electrode After Testing
(Image at ×50 magnification)

Figure 5.7 shows that ≈0.08 mm of the tip was burned off as a result of the ≈300 consecutive tests performed, however no significant carbon deposits where observed on the electrode surface.

a. The actual radius was checked under a microscope and found to be 0.44 mm.

With a fixed pressure of 200 kPa gauge (≈29.0 psig) chosen to be representative of practical apparatus operating pressures while at the same time conserving the usage of CF_4, a series of tests were conducted to establish the breakdown strength of SF_6-CF_4 mixtures under highly non-uniform field conditions. Two categories of tests were carried out independently, the results of which will be presented in detail in the following sub-sections. The first category of tests (Category A) consisted of applying voltage stresses to gap lengths of 10, 20, 25 and 30 mm. The voltage stresses applied were as follows:

1. Standard Lightning Impulse (≈1.2 × 50 μsec)
2. Positive Polarity dc
3. 60 Hz ac.

The second category of tests consisted of the following voltage stresses for gap lengths of 10, 20 and 30 mm:

1. Standard Switching Impulse (≈250 × 2500 μsec)
2. Positive Polarity dc and Corona Inception Measurement
3. 60 Hz ac and Corona Inception Measurement.

The purpose of repeating the positive polarity dc and ac breakdown voltage tests was twofold: first to ensure that the data measured in Category A was reproducible and second, to measure the onset of corona which was not performed in Category A. The circuit schematics and photographs of the above test setups have already been presented in Section 4.1 and will not be repeated here. Emphasis in this section is placed on the experimental results obtained from the testing and the trends that appear in the experimental data.

5.3.1 Category A Test Results:

The Category A tests commenced with filling the chamber to a pressure of 200 kPa with CF_4 C.P. grade (99.8%) and setting the gap length to 10 mm. The high voltage test circuits were arranged such that all three voltage types (impulse, dc and ac) were easily accessible, thus minimizing the down time between each test. For a test gap length, each type of voltage stress was applied in turn and upon completion of a set of tests, the gap was adjusted to a new length and the process repeated. Each gap length was "calibrated" by first establishing a zero gap with the use of an Ω-meter across the high voltage electrode and ground and then counting the number of

revolutions the earthed electrode made as the gap length was increased. Since the shaft of the earthed electrode was graduated in 5° increments, the resulting measuring error was no greater than 1 mm•(360° × 2)$^{-1}$ ≈ 0.0015 mm. Upon completion of the Category A tests, the 50% breakdown voltages and standard deviations were calculated as specified in Section 4.4, the data of which are presented in the following figures.

Figure 5.8 shows the results obtained from the standard lightning impulse tests with the 100%SF_6 and the 100%CF_4 curves defining respectively the upper and lower breakdown limits.

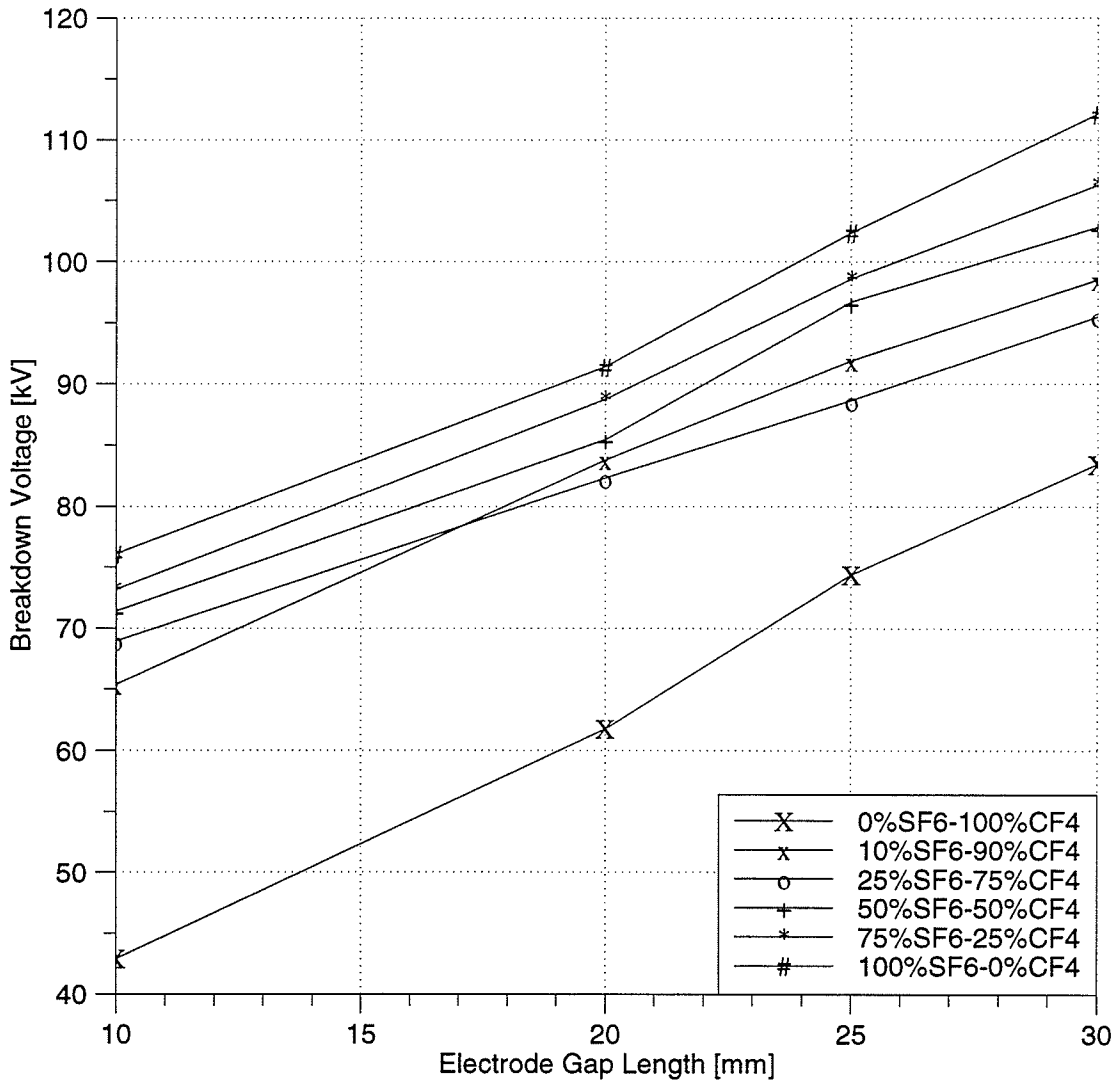

Figure 5.8
Standard Lightning Impulse Breakdown Voltages (Point (ϕ1.0 mm)-Sphere (ϕ62.5 mm), 200 kPa Pressure)

An interesting trend of these data are the initial sharp increases in breakdown voltage with the addition of the first 10% of SF_6 to CF_4. All further increases of SF_6 to the mixture reveal only a linear rise in breakdown voltage until the maximum is attained at 100% SF_6. Unfortunately, SF_6-CF_4 mixtures comprising less than 10%SF_6 per value were not investigated in this research. However it is evident that the dielectric strength of CF_4 which by itself is not much higher than N_2 for uniform fields, can be significantly improved by addition an incremental amount of CF_4.

The positive polarity dc breakdown voltage data are presented next in Figure 5.9.

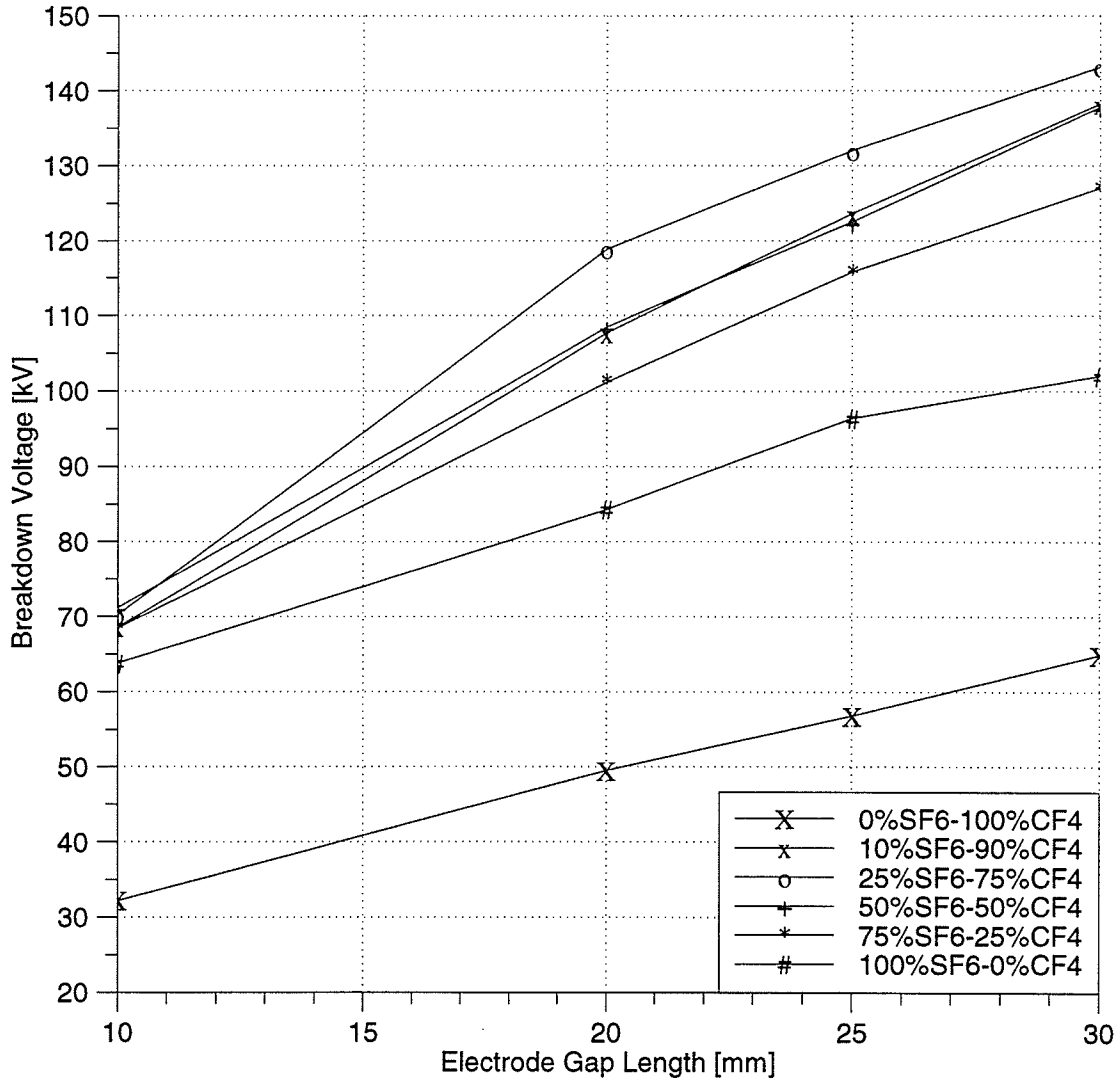

Figure 5.9
Positive Polarity dc Breakdown Voltages (Point (ϕ1.0 mm)-Sphere (ϕ62.5 mm), 200 kPa Pressure)

A noteable feature of these data is the strong positive synergism occurring in gap lengths ≥ 20 mm. Apparently as the field becomes increasingly divergent, the synergistic effect of the SF_6-CF_4 mixture becomes more prominent. A possible explanation of the mechanism at work here may lie in the fact that CF_4 has high electronegative properties for higher electron energies (typically ≥ 2.5 eV). As the field becomes more non-uniform the electrons, because of their high mobility are drawn towards the positive point and ionization by electron collision takes place in the high field region close to the point. As electrons are drawn towards the anode (point), the positive space charge left behind causes a reduction in the field strength close to the point while at the same time increasing the field further away from it. As the space charge propagates further into the gap the field strength at the tip of the space charge may be high enough to initiate a cathode-directed streamer which in SF_6 or CF_4 alone would lead to breakdown of the gap. However, for SF_6-CF_4 mixtures it appears that the electronegative CF_4 might attach to itself some of the high energy electrons thus greatly reducing the probability of a cathode directed streamer that would otherwise lead to a complete breakdown.

For the smallest gap length investigated (10 mm) a phenomenon similar to that observed under the lightning impulse voltages of Figure 5.8 is observed, namely a significant increase in dielectric strength by addition of the first 10% of SF_6 to CF_4. However, whereas 100%SF_6 defines the upper limit of breakdown voltage for the lightning impulses, for positive polarity dc the 100%SF_6 lies between the 100%CF_4 and the mixtures of SF_6-CF_4. At the time of this writing it is not known whether or not other researchers have investigated mixtures of SF_6-CF_4 under highly non-uniform field conditions, however an interesting paper was published in the late 1940's [20] which investigated the breakdown strengths of SF_6 and other fluorocarbons (individually) under highly divergent fields. Comparison of the breakdown data for 100%SF_6 and 100%CF_4 gathered during this thesis research with that of the data gathered in Reference 14 shows very good agreement. Unfortunately, due to time constraints and the limited supply of CF_4, testing at only a single pressure (200 kPa) was possible.

The ac data of Figure 5.10 show a similar breakdown voltage trend to that observed for the positive polarity dc, although the smallest gap length (10 mm) indicates no positive synergism as SF_6 is added to CF_4; the breakdown voltage data here are very similar to those of Figure 5.8.

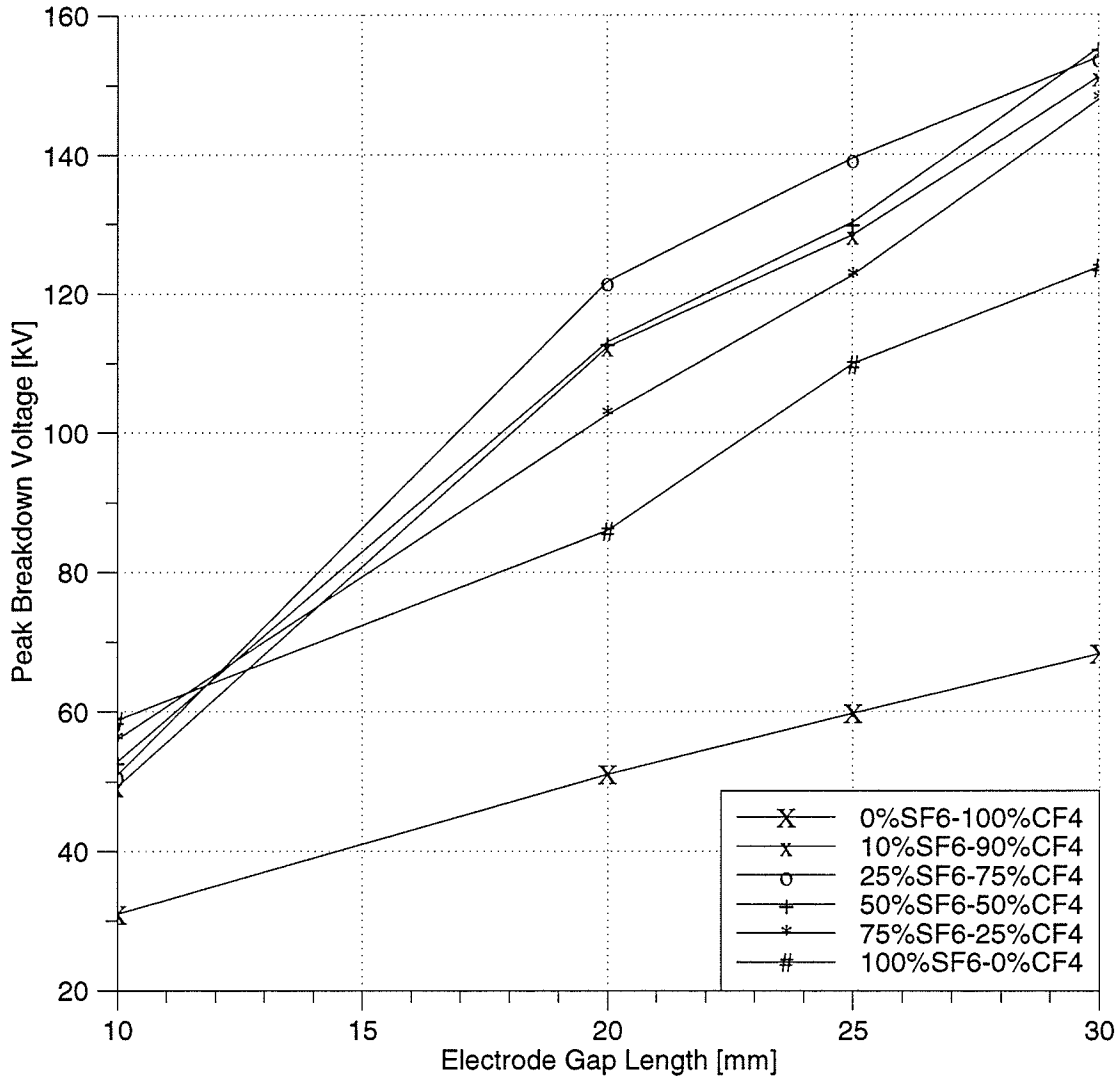

Figure 5.10
60 Hz ac Breakdown Voltages (Point (ϕ1.0 mm)-Sphere (ϕ62.5 mm), 200 kPa Pressure)

The ac breakdown voltage data share several similarities with the positive dc breakdown voltage data such as a large increase in breakdown strength after addition of the first 10% of SF_6 to CF_4, the highest breakdown voltage levels generally occurring for a mixture of 25%SF_6-75%CF_4 and the strong positive synergism occurring for increasing divergency of fields (gap lengths ≥ 20 mm). Figure 5.10 also shows that the breakdown voltage levels of ac are slightly higher than those for dc. This may be a result of particle accumulation inside the chamber due to the large number of breakdowns under which the electrodes were subjected. Under dc stress, these particles may have formed conduction paths which would not have occurred under the time varying ac stresses.

All data presented in Figures 5.8, 5.9 and 5.10 were plotted as breakdown voltage versus gap length. However, additional information can also be obtained by considering a single gap length and plotting breakdown voltage as a function of $\%SF_6$ per volume. For the Category A tests, two gaps lengths were selected: a 10 mm gap length the data for which is presented in Figure 5.11 and a 25 mm gap length for which data is shown in Figure 5.12. The 25 mm gap length was selected as a check for data validity. Testing was initially planned for only three gap lengths (10, 20 and 30 mm) but after observation of the large positive synergism activity occurring in highly divergent fields, it was considered worthwhile to include a fourth gap length.

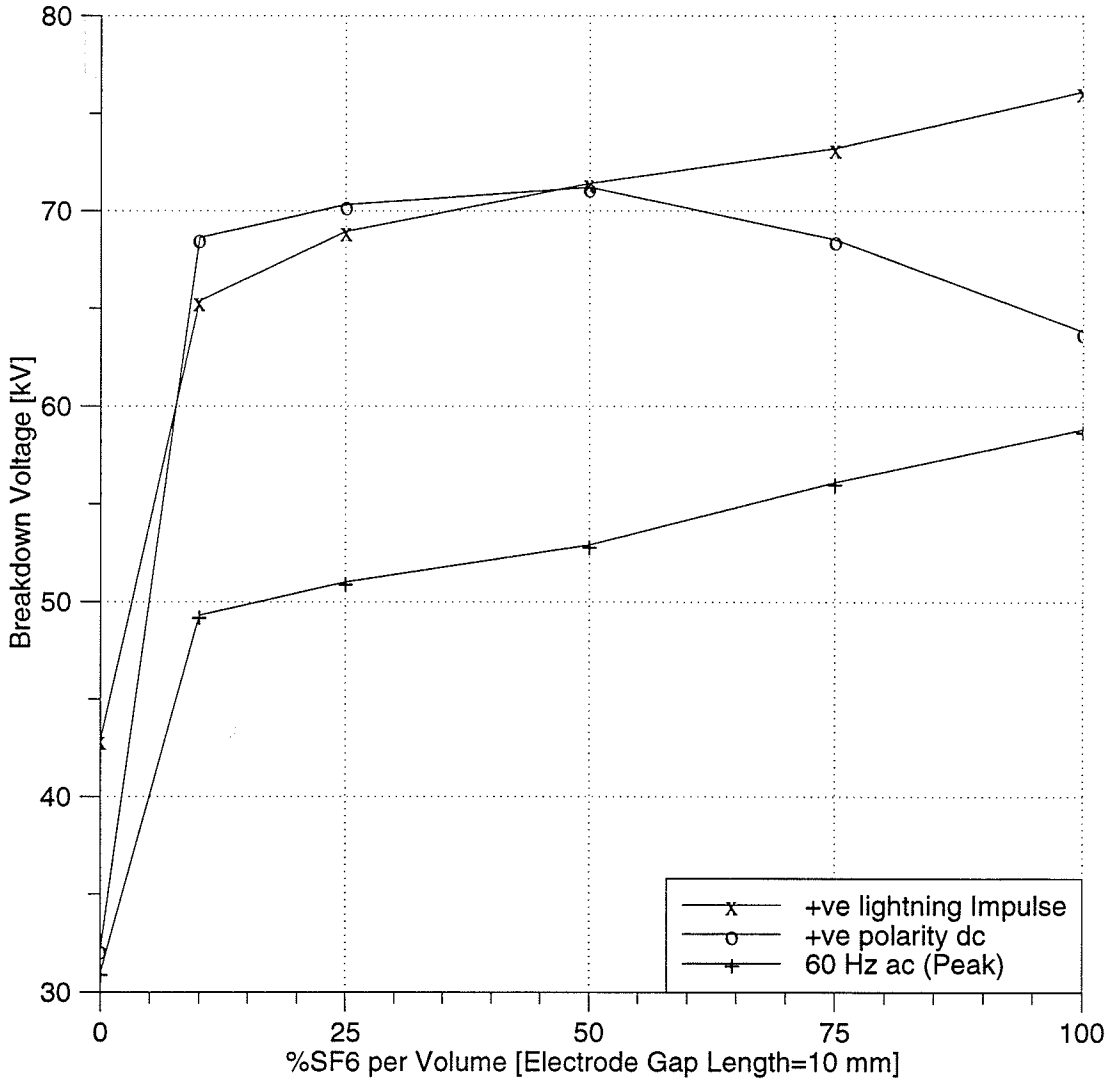

Figure 5.11
Breakdown Voltage as a Function of $\%SF_6$ (10 mm gap, 200 kPa pressure)

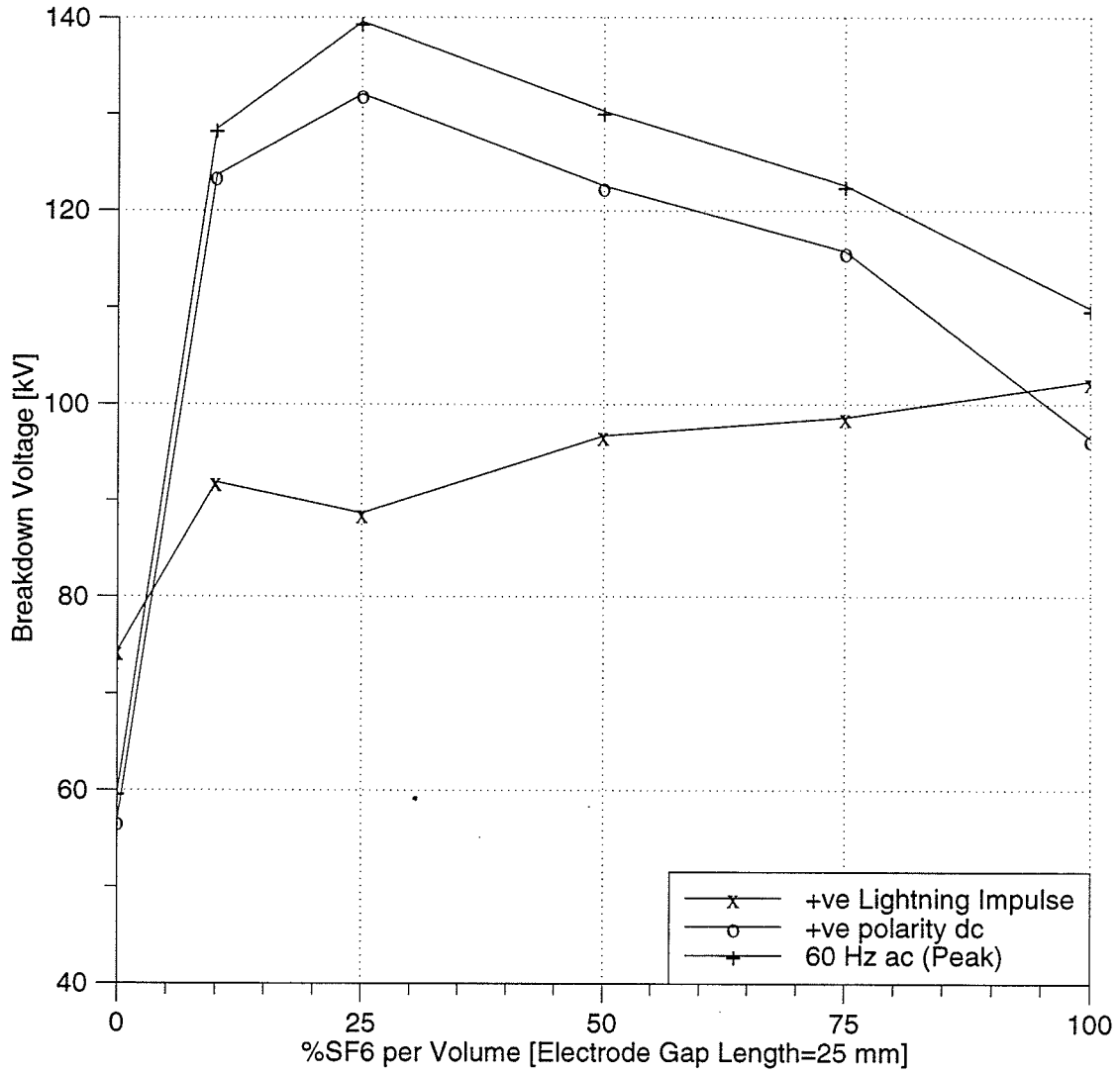

Figure 5.12
Breakdown Voltage as a Function of %SF_6 (25 mm gap, 200 kPa pressure)

The 10 mm gap length shows a higher initial increase in breakdown voltage with addition of the first 10% of SF_6 to CF_4. All subsequent additions of SF_6 to the SF_6-CF_4 mixture give a linear relation except for the low impulse breakdown voltage in the 25 mm gap length which could have been the result of asperities on one of the electrode surfaces or possibly an insufficient number of voltage applications.

Whereas the lightning impulse data show a relatively linear relation for all gap settings for SF_6-CF_4 mixtures containing $\geq$ 10%SF_6 per volume, the positive polarity dc and 60 Hz ac test

results show a definite positive synergism for all gap lengths with the largest breakdown values occurring for the ≈25%SF_6-75%CF_4 mixtures. Both Figures 5.11 and 5.12 reveal significant increases in breakdown voltages after the addition of the first 10% of SF_6 to CF_4 (≈60 kV increase for 25 mm gap). There is an anomaly associated with these data in that the dc breakdown voltage values are higher than those for ac in a 10 mm gap length though the ac breakdown voltage down values become higher than dc for a 25 mm gap length. An explanation of this behaviour might be that the time varying ac may increase the sensitivity of SF_6-CF_4 mixtures for small gap lengths whereas under dc stress the field remains relatively constant and increases only in intensity, finally breaking down from streamer propagation or particle accumulation in the gap. As the gap length is increased, the time varying ac may have less effect on the sensitivity of SF_6-CF_4 and since no particle accumulation can occur, the breakdown voltage values become higher than those for dc. As a validity check, the ac and dc breakdown voltage data for 100%SF_6 under highly non-uniform fields were checked with data by others [20,21,22,23] and found to be in very good agreement.

5.3.2 Category B Test Results:

Upon completion of the Category A tests, the test chamber was evacuated to a pressure of 0.0013 kPa (≈0.01 mm Hg), flushed with prepurified N_2 (99.995%) and then evacuated a second time to 0.0013 kPa. After a visual inspection of the point and sphere electrodes to ensure that they were both free from any defects, SF_6 of C.P. grade (99.8%) was admitted until a chamber pressure of 20 kPa was attained. CF_4 of C.P. grade (99.8%) was then admitted until a 200 kPa chamber pressure was attained giving a mixture of 10%SF_6-90%CF_4.

As was stated in Section V.3 the main purpose of this final phase of testing was to obtain data for standard switching impulse voltage stresses though it was later found worthwhile to repeat the positive polarity dc and 60 Hz ac tests not only for confirmation of data validity but also to measure the onset of corona (corona inception). Unfortunately, time constraints prevented the investigation of the 25 mm gap lengths and tests for only three gap lengths were performed (10, 20 and 30 mm). Also testing was not performed in 100% CF4 as there was not a sufficient supply of this gas to fill the chamber to a pressure of 200 kPa. The same measuring technique used for the lightning voltage tests were used for the switching voltage tests (see Figure 5.13 for data).

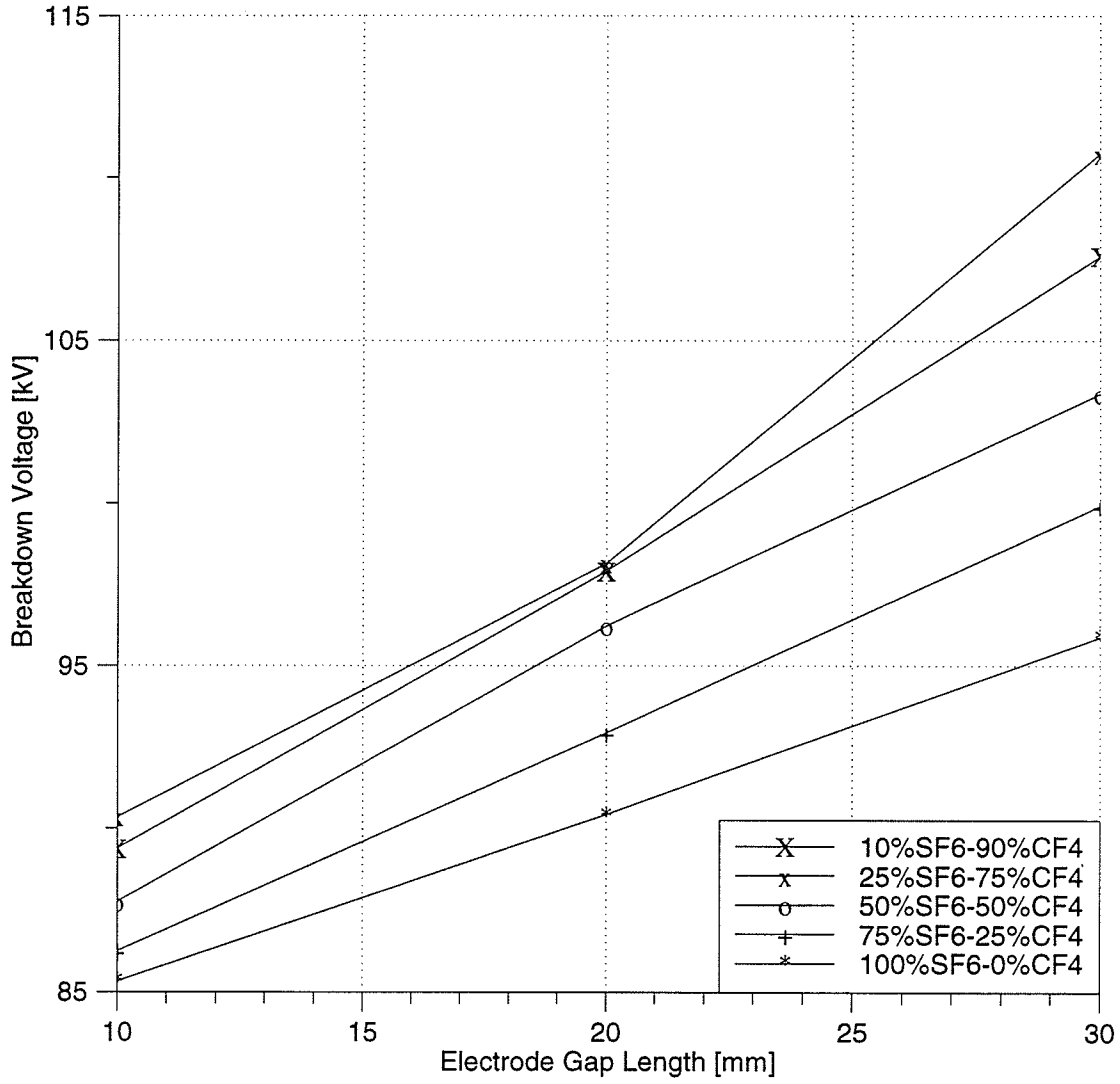

Figure 5.13
Standard Switching Impulse Breakdown Voltages (Point (ϕ1.0 mm)-Sphere (ϕ62.5 mm), 200 kPa Pressure)

These data show trends that are in very good agreement with the Category A positive polarity dc and 60 Hz ac results. Figure 5.13 gives indication of a strong positive synergism that holds for all three gap settings, although at a gap length of 30 mm the breakdown voltages diverge somewhat from the data measured for the 10 mm and 20 mm gap lengths. As with the lightning voltage tests, the breakdowns in each mixture for switching surge tests increases linearly with increasing gap length. The main difference is for the lightning voltage tests, 100%SF_6 defined the upper limit of breakdown strength whereas for ac, dc and switching surge tests, 100%SF_6 breakdown is the lowest of all SF_6-CF_4 mixtures (with the exception of 100%CF_4).

Breakdown voltages under highly non-uniform fields of various gap lengths are presented in Figures 5.14 and 5.15. The Category B tests also included corona inception voltages. The strong synergism that is evident in the Figure 5.9 test is again observed in Figure 5.14. 100%SF_6 has the lowest breakdown voltage except at the 10 mm gap where it has the highest breakdown voltage (with the exception of 100%CF_4). An anomaly observed in the data of Figure 5.14 are the unusually low breakdown values observed for 75%SF_6-25%CF_4 and 100%SF_6 at the 20 mm gap setting. This phenomenon may be a result of particle accumulation due to the time invariant voltage stresses.

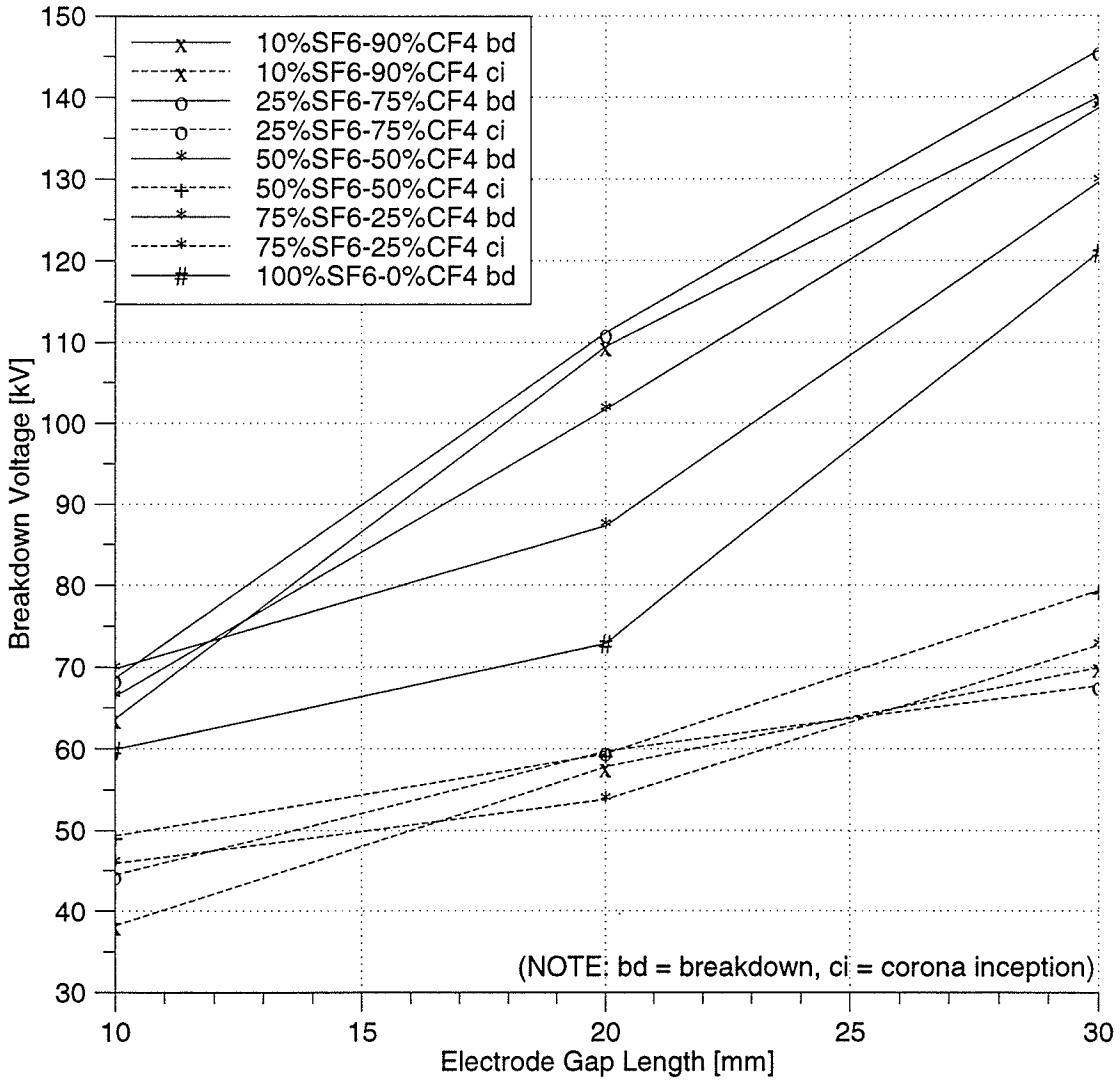

Figure 5.14
Positive Polarity dc Breakdown Voltages (Point (ϕ1.0 mm)-Sphere (ϕ62.5 mm), 200 kPa Pressure)

Figure 5.15 shows 60 Hz ac breakdown voltage data for gap lengths of 10, 20 and 30 mm. Inspection of these breakdown voltages shows good agreement with data obtained in Category A. A positive synergism effect is observed everywhere except in the 10 mm gap length where the breakdown voltages of 75%SF_6-25%CF_4 and 100%SF_6 seem unusually high. Conversely, these same mixtures have unusually low values for the 20 mm gap length, although this may be the result of particle contamination or a slight degradation of the gas. The corona inception voltages for both Figures 5.14 and 5.15 follow closely the trends of the breakdown voltage curves and are in good agreement with non-uniform field theory.

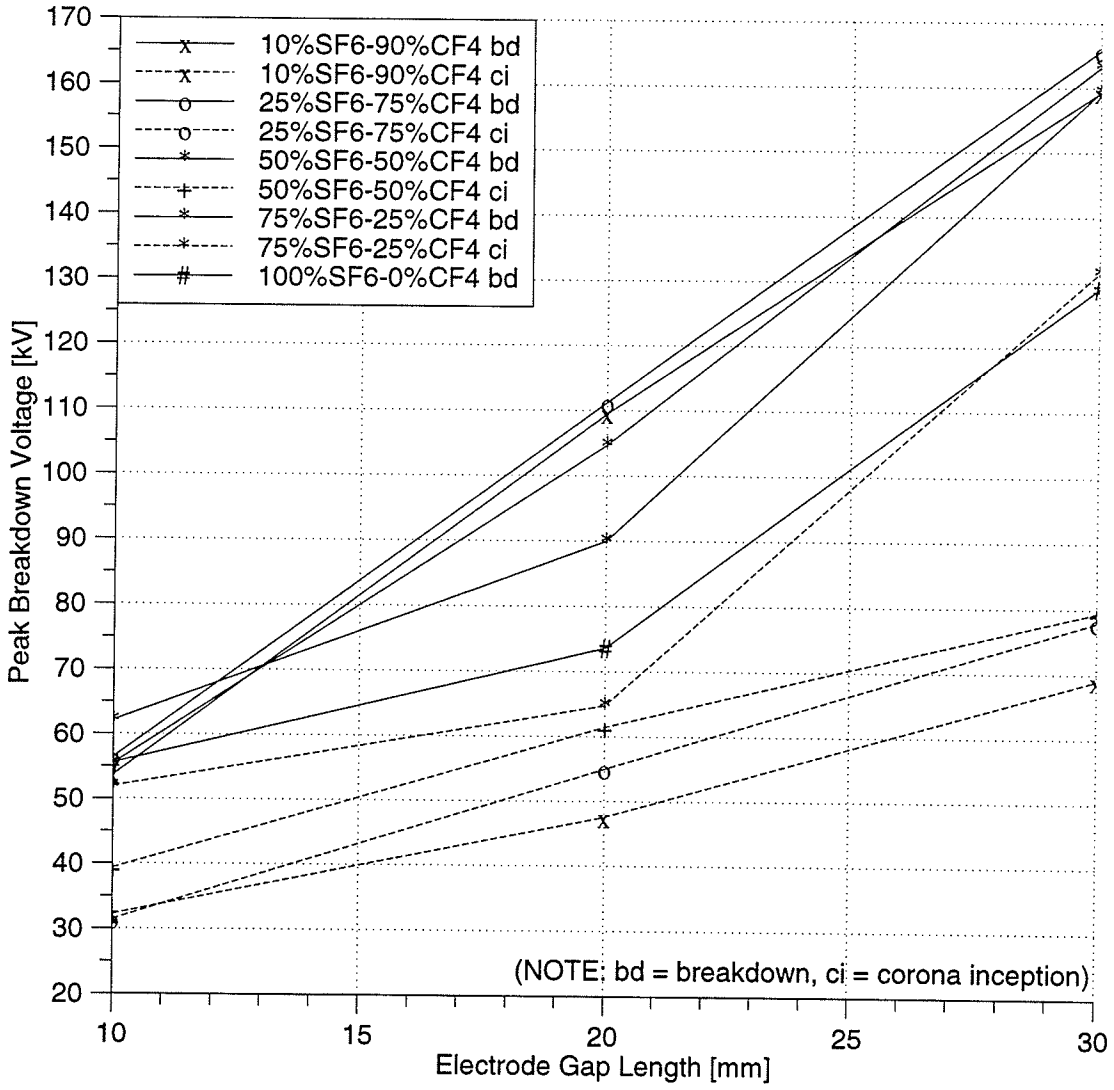

Figure 5.15
60 Hz ac Breakdown Voltages (Point (ϕ1.0 mm)-Sphere (ϕ62.5 mm), 200 kPa Pressure)

Figures 5.16 and 517 show respectively the breakdown voltage as a function of $\%SF_6$ per volume for gap lengths of 20 and 30 mm. The data are in good agreement with the results obtained from the Category A tests and for both gap lengths the ac breakdown voltage values are slightly higher than those for positive dc. It is speculated here that the dc breakdown values are lower due to particle accumulation in the gap under static field conditions. This would appear logical since after installation of the Point-Sphere electrodes, the chamber was not opened again until all highly non-uniform field tests were completed (≈300 separate tests). This would be ample time for sufficient particle build up within the chamber.

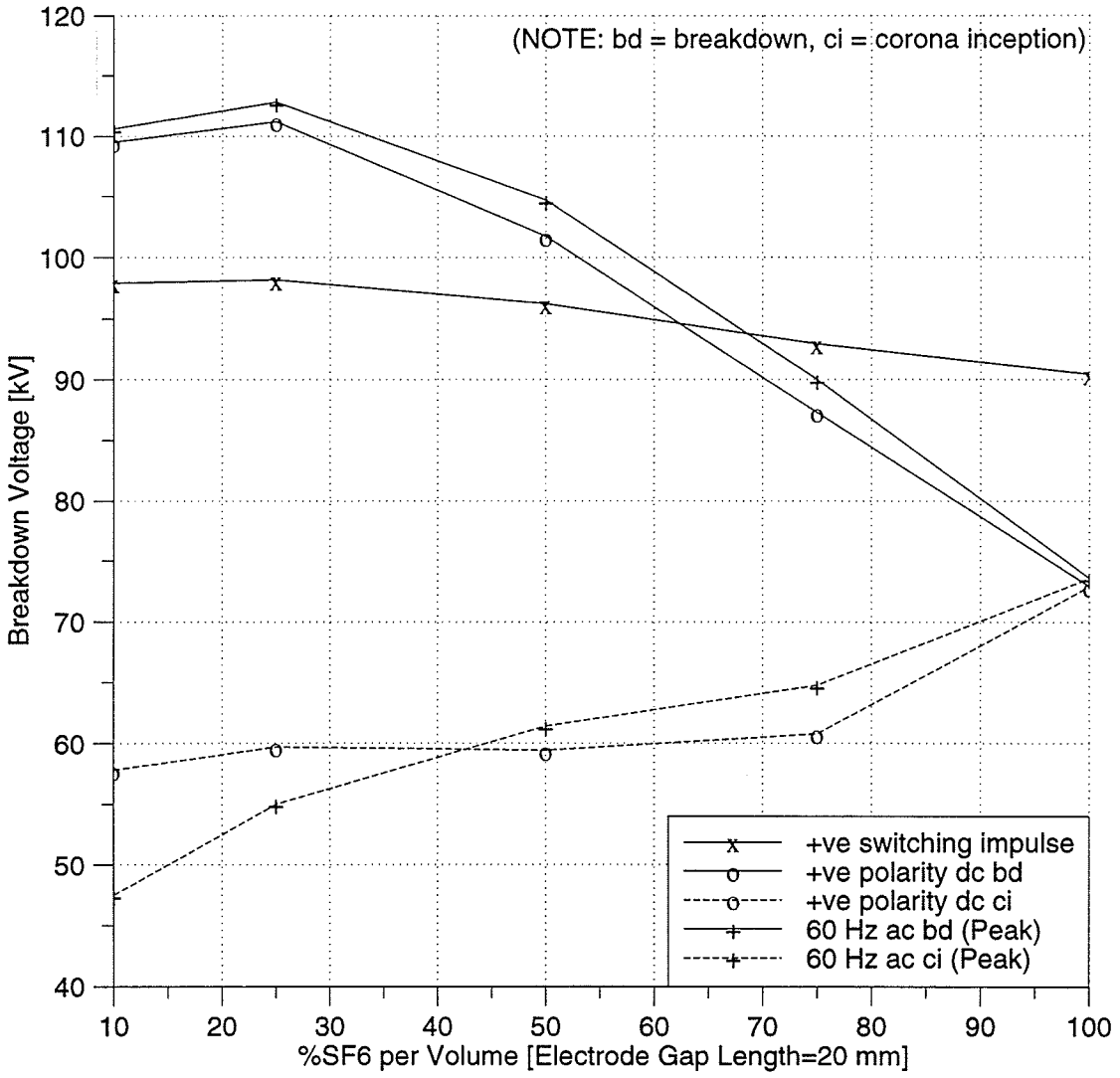

Figure 5.16
Breakdown Voltage as a Function of $\%SF_6$ (20 mm gap, 200 kPa pressure)

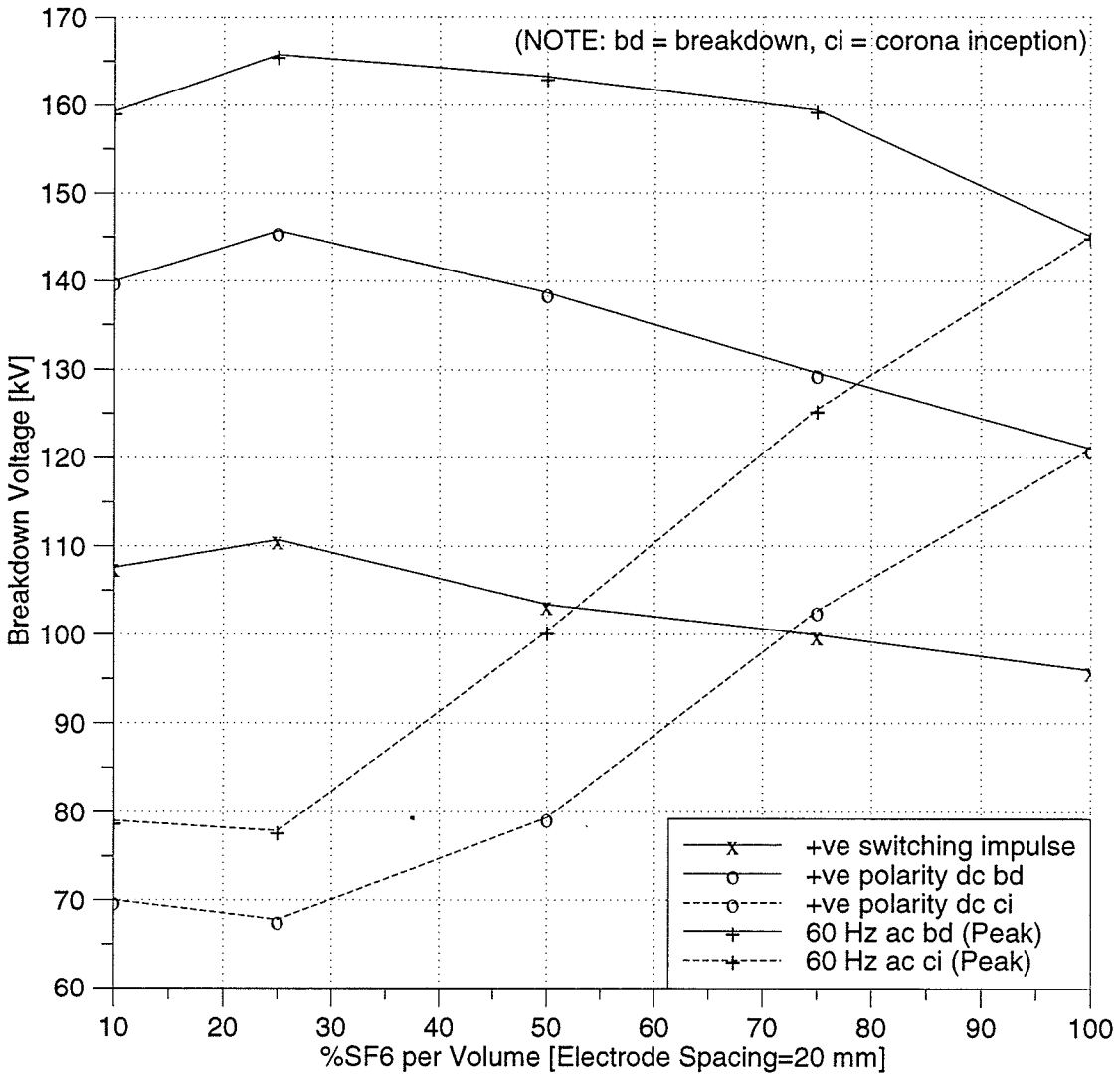

Figure 5.17
Breakdown Voltage as a Function of %SF_6 (30 mm gap, 200 kPa pressure)

Inspection of Figures 5.16 and 5.17 show the breakdown voltage and corona inception voltage values to be identical for 100% SF_6. For purposes of plotting these values were set equal to eachother; this is a valid assumption as previous tests of pure SF_6 under positive stress in non-uniform fields performed by others show that at pressures of ≈200 kPa the corona inception and gap breakdown occur at approximately the same voltage [3,23]. In fact, experiments carried out in pure SF_6 have shown that the region of corona stabilized breakdown under positive voltage is limited to pressures below ≈150 kPa. The data of Figures 5.16 and 5.17 confirm these observations since no indication of a corona could be detected for 100%SF_6 in any gap length.

6. CONCLUSIONS AND RECOMMENDATIONS FOR FUTURE WORK

The work presented in this thesis was undertaken to investigate the dielectric properties of SF_6-CF_4 mixtures under pressures and field geometries typical of those found in engineering applications. Breakdown voltage characteristics of various mixtures of SF_6-CF_4 were experimentally evaluated for standard lightning and switching surges as well as for positive polarity dc and 60 Hz ac voltages under various field geometries ranging from uniform to highly non-uniform. Since high voltage breakdown of any insulation invariably occurs at its weakest location, an exhaustive amount of experimental work was performed under highly non-uniform electric fields which would be representative of surface irregularities or corners found in practical apparatus.

Under uniform and quasi-uniform fields the breakdown voltages of SF_6-CF_4 mixtures varied linearly as a function of $\%SF_6$ per volume. However, under highly non-uniform fields a positive synergism was observed (the difference in the measured breakdown voltage of a particular mixture and the partial pressure weighted breakdown voltages of the component gases) for positive polarity dc and ac as well as to a limited degree with the standard switching surges. No synergism was evident under standard lightning impulse voltages perhaps due to an insufficient amount of time for the establishment of space charge within the gap which may be necessary for the formation of a corona stabilization.

Overall, the results presented in this thesis appear very interesting and despite the limited scope of the tests, seem to support the reason that several switchgear manufactures have chosen to use SF_6-CF_4 mixtures as gaseous dielectrics. Although it has been experimentally established elsewhere that SF_6-CF_4 mixtures, in particular mixtures comprising $50\%SF_6$-$50\%CF_4$ have superior arc quenching properties in comparison to SF_6-N_2 mixtures and a liquifaction temperature comparable to that of liquid N_2, this research has further revealed SF_6-CF_4 to have good dielectric properties under highly non-uniform fields. Despite the fact that the breakdown voltage of $100\%CF_4$ is quite low (comparable to the breakdown strength of air), upon addition of $\approx 10\%$ of SF_6 to CF_4 the resulting dielectric strength was observed to increase substantially and reached a maximum breakdown strength at a mixture of $\approx 25\%SF_6$-$75\%CF_4$.

A summary of the important observations noted during the course of this thesis are highlighted below:

- Gas mixtures require sufficient mixing times if stable breakdown data is to be obtained. A mixing fan greatly reduces the amount of necessary mixing time and eliminates the problem of gas layering.
- SF_6-CF_4 mixtures under uniform fields have breakdown voltages that vary linearly with respect to $\%SF_6$ content. Lightning impulse and ac stresses breakdown the mixture at similar magnitudes.
- SF_6-CF_4 mixtures under quasi-uniform fields follow the same linear relation in breakdown voltages as a function of $\%SF_6$ content. ac and positive polarity dc stresses are comparable but are substantially lower than lightning surge breakdowns.
- Under highly non-uniform fields, a strong positive synergism occurs under ac, positive dc and standard switching voltages for the mixtures $10\%SF_6$-$90\%CF_4$ to $25\%SF_6$-$75\%CF_4$. No synergism is observed for standard lightning voltages.
- Corona inception voltage curves follow similar trends to those of the corresponding breakdown voltages. Corona inception voltage for $100\%SF_6$ is indistinguishable from the breakdown voltage at a pressure of 200 kPa.
- Breakdown voltages are observed to decrease in magnitude after a gap is subject to a large number of breakdowns (especially under dc stresses) perhaps due to particle contamination or gas degradation.
- Inspection of chamber and electrode surfaces reveals negligible carbon deposits after $\approx$300 individual tests of various SF_6-CF_4 mixtures.

Some recommendations for future work which would complement what has already been performed include:

- Breakdown studies under quasi-uniform fields for varying gap lengths.
- SF_6-CF_4 mixtures under various stresses tested for breakdown voltage as a function of pressure (for pressures of 100-500 kPa).
- Determine analytically and experimentally the effective window of electron attachment for SF_6-CF_4.

- Investigate the formation of space charge in SF_6-CF_4 mixtures and how it affects the breakdown strength under different voltage stresses.
- Study the arc quenching properties of SF_6-CF_4 and determine how this changes with successive breakdowns.
- Conduct a time lag study of breakdowns and plot the corresponding volt-time characteristics.
- Test the dielectric integrity of SF_6-CF_4 mixtures under fast transients and chopped impulse surges.

Finally, it is sincerely hoped that these experimental data will be useful in future studies, not only in the field of high voltage research but also as practical data that may be used to embellish existing designs in power apparatus such as switchgear, circuit breakers and dry transformers. From a review of the literature, it has been observed that virtually no research work exists which considers exclusively the dielectric properties of SF_6-CF_4 mixtures. Provided the Canadian government realizes that CF_4 is indeed a non-Freon gas and removes the generic name Freon-14 from it, then perhaps the results this thesis will spawn an interest into future investigations of this practical insulation.

References

1. H. Moissan and P. Lebeau, Component Review, Vol. 130, pg. 180, 1900.

2. F. Cooper, "Gas Insulated Device", U.S. Patent No. 2 221670, 1940.

3. E. Kuffel and W. Zaengl, "High Voltage Engineering Fundamentals", Pergamon Press, Oxford, Eng., 1984.

4. F. Clark, "Insulating Materials for Design and Engineering Practice", John Wiley and Sons, Inc., New York, U.S., 1962

5. L. Christophorou, D. James and R. Pai, "Applied Atomic Collision Physics", Vol. 5, pp. 87-167, 1982.

6. D. Bouldin, D. James, M. Pace and L. Christophorou, "A Current Assessment of The Potential of Dielectric Gas Mixtures for Industrial Application", Gaseous Dielectrics IV, pp. 204-212, Pergamon Press, New York, U.S., 1984.

7. L. Christophorou, I. Sauers, D. James, H. Rodrigo, M. Pace, J. Carter and S. Hunter, "Recent Advances in Gaseous Dielectrics", IEEE Int. Sym. on Elect. Insul., pp.122-136, Montreal, Ca., June 11-13, 1984.

8. BNL-51719, Power Transmission Project Technical Note 138, Division of Advanced Applications, Accelerator Department, Brookhaven National Laboratory, Upton, NY, 1983.

9. S. Rigby and B. Weedy, "Partial Discharges in Liquid Nitrogen Impregnated Taped Cable Insulation", Proceeding of IEE, Vol 123, No. 2, pp. 165-170, 1976.

10. K. Horii, "Correlation of Electrical Breakdown of Supercritical Helium in Short Gaps with Partial Discharge in Cable Samples", Cryogenics, pp. 102-106, 1993.

11. R. Middleton, V. Koschik, P. Hogg, P. Kulkarni and H. Heiermeirer, "Development Work for the Application of 245 kV Circuit Breakers Using a SF_6-CF_4 Gas Mixture on the Manitoba Hydro System", CEA Conf., Toronto, Ca., March, 1994.

12. G. Camilli and R. Plump, "Fluorine Containing Gaseous Dielectrics", AIEE Trans., Vol. 72, Part I, pp. 93-102, 1953.

13. G. Camilli, T. Liao and R. Plump, "The Dielectric Behavior of Some Fluorogases and Their Mixtures", AIEE Trans., Vol. 74, Part I, pp. 637-642, 1955.

14. C. Works and T. Dakin, "Dielectric Breakdown of Sulphur Hexafluoride in Nonuniform Fields", AIEE Trans. Vol. 72, Part I, pp. 682-687, 1953.

15. D. Berg and C. Works,"", AIEE Trans. on PAS, Vol. 77, pg 820, 1958.

16. M. Abou-Seada and E. Nasser, IEEE Proc., Vol. 56, pg. 813, 1968.

17. Z. Li and C. Zhang, "Measurements of Synergisms of Strongly Electronegative Gaseous Mixtures", Proc. of 7th Int. Sym. on Gas. Diel., Knoxville, Tenn., April 24-28, 1994.

18. IEC 60-1, "High Voltage Techniques", Geneve, Sw., 1989.

19. Z. Li, "The Breakdown Voltage-Time Characteristics of SF_6 and its Mixtures in Coaxial Cylinder Gaps with Special Reference to Steep-Fronted Impulse Voltages with Time to Chopping Down to 100 nsec", PhD Thesis, University of Manitoba, 1989.

20. G. Camilli and J. Chapman, "Gaseous Insulation for High-Voltage Apparatus", AIEE Tans., Vol. 66, 1947.

21. Y. Qiu, Y. Feng, C. Lu and Z. Wu, "Breakdown of SF_6 and Some SF_6 Mixtures in a Point-Plane Gap", 7th ISH, Paper No. 32.09, pp. 83-85, Dresden, August 26-30, 1991.

22. Y. Qiu and E. Kuffel, "Dielectric Strength of Gas Mixtures Comprising SF_6, CO, c-C_4-F_8 and SF_6, N_2, c-C_4F_8", IEEE Trans. on PAS, Vol. PAS-102, No. 5, pp. 1445-1450, May 1993.

23. V. Maller and M. Naidu, "Advances in High Voltage Insulation and Arc Interruption in SF_6 and Vacuum", Pergamon Press, Oxford, Eng, 1981.

Appendix A

The Free Path of Molecules and Electrons

Knowledge of the physical dependency and distribution of free paths l may offer a simplified explanation of the dependency of $\alpha = f(E,N)$ as defined in Section 2.4. Using an elementary ballistic model, λ can be defined as the distance a molecule or particle travels between collisions. It should also be noted that l is a statistical quantity and its mean value (mean free path $\overline{\lambda}$) depends upon the concentration of particles or the density of a particular gas.

By assuming an assembly of stationary molecules of radius r_1 and a moving layer of smaller particles of radius r_2 (see Figure A.1), a derivation of λ may be formulated. From molecular physics, as the smaller particles move, their density will decrease due to scattering caused by collisions with the larger gas molecules. By considering the moving particles and molecules to be of spherical geometry, then a collision will occur every time the centre of two particles come within a distance $r_1 + r_2$ of eachother as can be seen in Figure A.1.

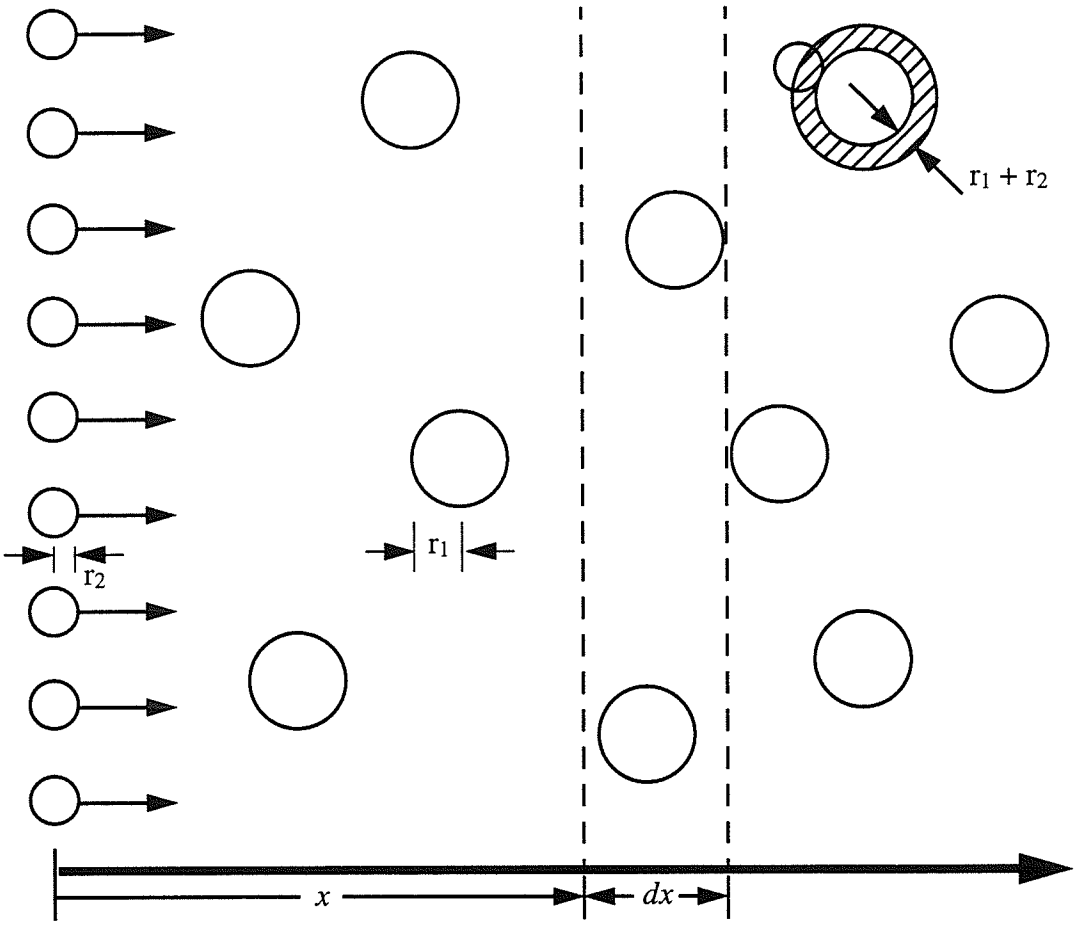

Figure A.1
Elementary Ballistic Model for Determining Free Paths

Now if $r_1 + r_2$ is the effective distance of collision then $\pi(r_1 + r_2)^2$ must be the effective area of interception of a particular gas. A more general definition for the effective area of interception in a unit volume of gas would be $N\pi(r_1 + r_2)^2$ where N is defined as the number of particles per unit volume of gas.

Referring to Figure A.1, a layer of thickness dx is chosen a distance x from the origin. If $n(x)$ is defined as the number of particles that travel a distance x from the origin with no collision, then the decrease in moving particles due to scattering in layer dx will be

$$dn = -n(x) N\pi (r_1 + r_2)^2 dx \qquad \text{A.1}$$

If the initial concentration of particles at $x = 0$ is no, then the deferential Equation of A.1 can be solved by Separation of Variables:

$$\int_{n_o}^{n(x)} \left(\frac{1}{n}\right) dn = -\int_0^x N\pi (r_1 + r_2)^2 da$$

$$\therefore n(x) = n_o e^{-N\pi (r_1 + r_2)^2 x} \qquad \text{A.2}$$

Now the probability of $\lambda = x$ will be equal to the probability of collisions between x and $x+dx$.

To verify the relation $\lambda = x$, Equation A.2 must first be differentiated with respect to x which gives:

$$f(x) = d\left(\frac{n}{n_o}\right) = N\pi (r_1 + r_2)^2 e^{-N\pi (r_1 + r_2)^2 x} dx \qquad \text{A.3}$$

But $f(x)$ is a continuous random variable which may be used to evaluate the expected value (ensemble average or mean). Since x is a linear operator, the following relation will hold true:

$$\bar{x} = \bar{\lambda} = \int_{-\infty}^{\infty} x f(x)\, dx$$

$$= N\pi (r_1 + r_2)^2 \int_0^{\infty} x e^{-N\pi (r_1 + r_2)^2 x}\, dx$$

$$= \frac{1}{N\pi (r_1 + r_2)^2} \qquad \text{A.4}$$

Since $\pi(r_1 + r_2)^2$ has the dimensions of area, Equation A.4 may be equivalently written as:

$$\sigma = \frac{1}{N\bar{\lambda}} \qquad \text{A.5}$$

where: $\sigma = \pi(r_1 + r_2)^2 \equiv$ effective cross-section of interception.

It should be noted here that the effective cross-section of ionization a may be defined by similar techniques and that the simple collision model presented here may be used to help explain processes such as ionization, excitation, attachment, etc.

Appendix B

Detailed Model of a Typical Gas Insulated Switchgear Design

B.1 GIS Design Criteria and Illustrative Model:

To give the reader some insight into the design of typical Gas Insulated Switchgear (GIS), a working model is presented here to illustrate some important aspects of GIS. In order to simplify the construction and conform to the many existing substation layouts, the elements of the switchgear and the bus are typically of single phase design and construction as can be seen in the GIS cross-section model of Figure B.1.

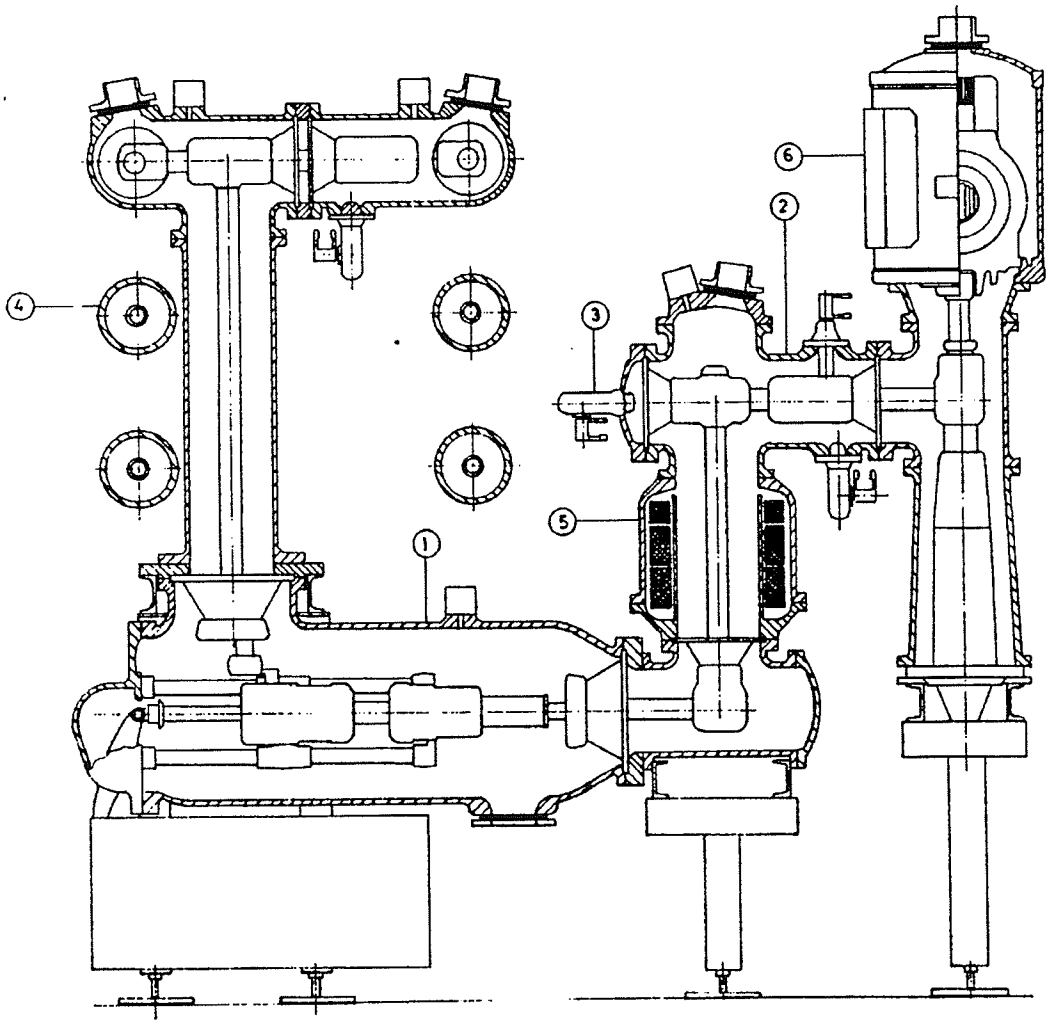

Figure B.1
Cross-Sectional View of a 170 kV Gas Insulated Switchgear Apparatus

The SF_6-N_2 or SF_6-CF_4 gas mixture is usually at a working pressure of 200-500 kPa though at atmospheric pressure the system is generally designed to withstand the rated phase to ground voltage. The metallic sheath is made out of aluminium to minimize eddy current losses at higher ratings ($\geq$ 2 kA) or steel with non-magnetic inserts placed to reduce eddy current heating. The bus conductors and bolted connectors are generally made of aluminium although copper is always used for the switch and circuit breaker contacts. Earthing is provided by solidly grounding the entire enclosure and automatic switches are employed for additional grounding of the cable whenever the isolators are operated. Finally, in order minimize the loss of gas due to failure of any one piece of equipment, a gas tight modular design is adopted and each module is provided with safety discs which rupture at a preset pressure and prevent any pressure build up on the enclosure. Gas monitoring pressure switches are also provided which will operate in the event of a leak.

B.2 Modular Layout of GIS:

Figure B.1 shows the general layout of a 170 kV GIS developed by Spreecher and Schuh and is comprised of a circuit breaker, isolators, earthing switch, busbars and current and voltage transformers. A brief description of each of these individual components or modules is discussed next.

B.2.1 Circuit Breaker:

A single pressure interrupter with one break per phase is employed as a power circuit breaker. Each phase of the breaker is typically provided with one motor wound spring operating mechanism suitable for rapid auto-reclosure. When a trip command is received, an electromagnetically operated trip valve opens so that high pressure gas flows into the lower part of the interrupter unit forcing a piston carrying the moving contact upwards to the open position. The gas flows through nozzles in the fixed contact so that the gas is directed against the arc almost at right angles which de-ionizes the arc channel at current zero and establishes a high dielectric strength at the break. To close the breaker, a closing valve is opened which admits high pressure gas above the piston. Operating pressure inside the breaker is approximately 630 kPa @ 20 °C.

B.2.2 Isolator:

The isolator is of a push-pull design which again functions as a single phase unit. The working part is comprised of a fixed contact and a spring contact, both of which are held in position by supporting insulators and a rotating insulation rod. A common motor operating mechanism drives the rotating insulating rod and the sliding contacts of the three phases are connected to them through an operating rod located outside the enclosure. A high speed grounding switch can also be attached to the isolators.

B.2.3 Earthing Switch:

The earthing switch is designed as a module for mounting on other apparatus. It is a mechanism comprised of built-in secondary contact fingers and a moving contact rod which is driven through a linkage system. High speed earthing switches are used for the operational earthing of parts of substations. These switches are triple pole driven by one motor-wound spring operating mechanism and can be switched on to short circuit faults.

B.2.4 Busbars:

The single phase busbar element comprises a conductor and cylindrical enclosure with an expansion bellows. The conductors of the two sections are connected to eachother by means of plug-in contacts. Changes in the length of the conductor due to temperature gradients are compensated by these contacts. Earthing switches and voltage transformers can be fitted at the ends of the busbars.

B.2.5 Voltage Transformer:

Encapsulated magnetic or capacitive voltage transformers (VTs) are used depending upon the voltage rating of the system. The active part of the magnetic VT is comprised of a closed iron core that supports the secondary and high voltage windings. Depending on the rated voltage, the high voltage insulation consists of cast resin or an SF_6 impregnated plastic film insulation. Each single phase VT constitutes a separate gas compartment equipped with a protective disc.

B.2.6 Current Transformer:

Metering and protection type current transformers (CTs) are generally of an encapsulated design. The CT essentially consists of a central circular conductor which acts as the primary winding and a concentric secondary winding wound around toroidal cores. A non-magnetic screening is usually provided just inside the secondary cores and the secondary connections are brought to a secondary terminal box through a bushing plate.

The design of any switchgear item or system is generally made on the basis of some empirically derived equations and from experience. As with any high voltage equipment, efficient design requires a knowledge of the maximum voltages the equipment may be subject to during its operational life and should be able to withstand these stresses without any damages. Some typical voltage stress tests may include:

- Standard impulse voltage as a criterion for stresses imposed by atmospheric over voltages.
- Power frequency voltage as an aggravated simulation of the over voltages experienced under normal operating conditions.
- Switching surges to prove the ability of the dielectric to withstand over voltages caused by switching operations.
- Increased service voltage to prove freedom from internal discharges so as to ensure that in service, there can be no progressive deterioration of insulation.

In addition, it is commonly specified that for worst case situations the dielectric strength of the system in service shall be assured when the internal gas pressure drops to atmospheric.

Appendix C

An Example of the Test Chamber Filling Procedure

Because the dielectric strength of a particular gas mixture can vary substantially with only an incremental change in the volumetric proportions of the individual constituents, great care must be taken when administering a mixture into a pressure vessel to ensure high accuracy is maintained. As was mentioned in Section 4.3 a Matheson pressure gauge with a measuring error of ±0.25% was used during the chamber filling process. For any particular test, after the chamber had been evacuated to 0.0013 kPa (≈0.01 mm Hg), the smallest constituent gas was administered first, followed by the larger constituent gas.

For example, suppose a 25%SF_6-75%CF_4 mixture @ 200 kPa (≈29.00 psig) were required. SF_6 would be first administered into the chamber (after purging all air out of the pressure line) until the gauge pressure reads 50 kPa. CF_4 would next be administered into the chamber until the gauge pressure reads 200 kPa. Prior to any testing, the mixing fan inside the chamber would be activated and the gases allowed to mix for at least one hour. After completion of testing for a particular mixture, suppose it is required to perform testing on a 50%SF_6-50%CF_4. Instead of purging the chamber and administering a new mixture which would not only be time consuming but also very wasteful of gases, the following procedure was followed which maximizes the conservation of gas supplies and minimizes the amount of down time.

STEP 1: Calculate individual gas proportions based on total pressure[a]:

$$29.00755 = 7.25189 + 21.75566.$$

STEP2: For a resulting mixture of 50%SF_6-50%CF_4 the new pressure of SF_6 must increase to 14.50377 from 2.41730 psig. Similarly CF_4 must decrease from 21.75566 to 14.50377 psig. Thus a total pressure of 7.25189/0.75 = 9.66919 psig must be bled from the chamber. Finally a 9.66919 psig of SF_6 must be administered to bring the total pressure up to ≈29.00 psig; the resulting mixture will then be 50%SF_6-50%CF_4 mixture @ 200 kPa. Mathematically, the mixing procedure is as follows:

29.00755	=	7.25189	+ 21.75566	(25%SF_6-75%CF_4)
		-2.41730	-7.25189	(bleed off)
		4.83459	14.50377	
		+9.66918	+0.00000	(fill with SF_6)
		14.50377	14.50377	(50%SF_6-50%CF_4)

a. Dimensions used for all pressure calculation were pounds per square inch gauge (psig)

Appendix D

Computer Program in C to Evaluate the Up and Down Method

The IEC 60-1 International Standards define the Up and Down method as a Class 2 statistical evaluation. In a Class 2 test, n groups of m substantially equal voltage stresses are applied at voltage levels U_i. The voltage level for each successive group of stresses is then increased or decreased by some incremental amount (typically ±3% of the reference stress) according to the result of the previous group of voltage stresses.

The procedure used to evaluate data obtained from the standard lightning and standard switching impulse tests can be thought of as a discharge procedure which finds voltage levels corresponding to high disruptive discharge probabilities. Here the voltage level is increased by some ΔU if one or more withstands occur, else it is decreased by the same amount. Tests with values of m other than 1 can be successfully used to determine voltages corresponding to other disruptive discharge probabilities. The results are the numbers k_i of stress groups applied at the voltage levels U_i. The first level U_i taken into account is that which at least two groups of stresses are applied. The total number of useful stress groups will then be $n = \Sigma k_i$.

After evaluating the 50% breakdown voltage and standard deviation by hand using the Up and Down criteria for a few sets of impulse data, it was quickly decided that it would be much more expedient to write a computer program to evaluate these data automatically. Using Appendix A of the IEC 60-1 International Standards as a reference, equations were formulated which could be used by the program to produce the 50% breakdown voltage and standard deviation.

The following source code is for a C program which first reads a file containing the data from a specific test (voltage stress applied at each shot, breakdown or withstand at each shot). The data are then sorted from lowest stress to highest stress and the number of distinct voltages levels are calculated. Finally the processed are applied to a set of equations that generate values of 50% breakdown voltage and standard deviation. Corrected values of these quantities are then calculated using the following relation:

$$V_{Corrected} = \left(\frac{Pressure\,[kPa]}{101.325\,[kPa]}\right) \cdot \left(\frac{295.15\,[K]}{Temperature\,[K]}\right) \cdot V_{50}.$$

```
/*****************************************************************************/
/***A PROGRAM TO DETERMINE THE MEAN AND THE STANDARD DEVIATION*************/
/***OF A SET OF STATISTICAL DATA USING THE UP AND DOWN METHOD*****************/
/**************(Last updated on March 13, 1995)*****************************/
/*****************************************************************************/

#include<stdio.h>
#include<math.h>

void main()

{

 FILE *fd1;

 char read_file[15];
 int temp,i,j,t,scroll,numsh,max;
 float temp1,temp2,temp3,lowv,numbd,numws,
     numj,deltv,N,A,B,coeff,V_50,stdev;
 float raw_dta[30][4],temp_dta[30][3],dta[30][3],
     swap1[1][3],swap2[1][3];
 float comp();

/*****************************************************************************/
/***OPEN AN EXTERNAL FILE AND READ RAW DATA*********************************/
/*****************************************************************************/

 printf("\nEnter name of data file to be read: ");
 scanf("%s",read_file);

 if((fd1=fopen(read_file,"r"))==NULL){

  printf("\nCould not open data file\n");
  exit(0);

 }

 numsh=0.0;
 i=0;
```

```
while(scroll=fscanf(fd1,"%d %f %f %f",&temp,&temp1,&temp2,&temp3)
    !=EOF){
 raw_dta[i][1]=temp1;
 raw_dta[i][2]=temp2;
 raw_dta[i][3]=temp3;
 raw_dta[i][4]=0.0;
 temp_dta[i][2]=0.0;
 temp_dta[i][3]=0.0;
 numsh+=(int)(temp2+temp3);
 i++;

 }

 fclose(fd1);

/*****************************************************************************/
/***DETERMINE NUMBER OF UNIQUE VOLTAGE STRESSES. IF A PARTICULAR*************/
/***VOLTAGE STRESS CONTAINS A GROUP, SET FLAG raw_dta[i][4]=1.0*****************/
/*****************************************************************************/

 for(j=0;j<=numsh-1;j++){

  for(i=0;i<j;i++){

   if(raw_dta[i][1]==raw_dta[j][1]){

    raw_dta[j][4]=1.0;
    i=j;

   }

  }

 if(raw_dta[j][4]!=1.0){

  temp_dta[j][1]=raw_dta[j][1];

  for(i=j;i<=numsh-1;i++){
```

```
 if((raw_dta[i][1]==raw_dta[j][1])&&(raw_dta[i][2]==1.0))

  temp_dta[j][2]+=1.0;

 if((raw_dta[i][1]==raw_dta[j][1])&&(raw_dta[i][3]==1.0))

  temp_dta[j][3]+=1.0;

 }

}else

 temp_dta[j][1]=0.0;

 }

/*****************************************************************************/
/***LUMP ALL GROUPS WITH SAME VOLTAGES TOGETHER*****************************/
/*****************************************************************************/

 j=0;

 for(i=0;i<=numsh-1;i++){

 if(temp_dta[i][1]!=0.0){

  dta[j][1]=temp_dta[i][1];
  dta[j][2]=temp_dta[i][2];
  dta[j][3]=temp_dta[i][3];
  j+=1;

 }else

  j=j;

 max=j;

 }
```

```
/*****************************************************************************/
/***SORT VOLTAGE STRESS DATA FROM LOWEST TO HIGHEST (Bubble Sort)**************/
/*****************************************************************************/
 do{

 t=0;

 for(i=0;i<max-1;i++){

  for(j=1;j<=3;j++){

   swap1[0][j]=dta[i][j];
   swap2[0][j]=dta[i+1][j];

  }

  if(comp(swap1[0][1],swap2[0][1])==1.0){

   for(j=1;j<=3;j++){

    dta[i][j]=swap2[0][j];
    dta[i+1][j]=swap1[0][j];
    t=1;

   }

  }else{

   for(j=1;j<=3;j++){

    dta[i][j]=swap1[0][j];
    dta[i+1][j]=swap2[0][j];

   }

  }

 }
```

```
}while(t==1);

/*****************************************************************************/
/***WRITE SORTED DATA TO AN EXTERNAL FILE FOR VERIFICATION*********************/
/*****************************************************************************/

fd1=fopen("sorted.dta","w");

deltv=dta[1][1]-dta[0][1];

for(i=0;i<=max-1;i++)

 fprintf(fd1,"%3.2f\t %1.1f\t %1.1f\n",
  dta[i][1],dta[i][2],dta[i][3]);

fclose(fd1);

/*****************************************************************************/
/***PERFORM UP AND DOWN METHOD TO DETERMINE MEAN AND STD. DEVIATION*************/
/*****************************************************************************/

numbd=0.0;
numws=0.0;

for(i=0;i<=max-1;i++){

 if((i>=1)&&((dta[i][1]-dta[i-1][1])<0.0)){

  printf("\nAn error occurred in the sorting routine\n");
  exit(0);

  }

 if((i>=1)&&(fabs(deltv-(dta[i][1]-dta[i-1][1]))>0.0001)){

  printf("\nAn error occurred in calculating deltv\n");
  exit(0);
```

```
}

numbd+=dta[i][2];
numws+=dta[i][3];

}

lowv=dta[0][1];
N=0.0;
A=0.0;
B=0.0;

if(numbd<numws){

 for(i=0;i<=max-1;i++){

  numj=dta[i][2];
  N+=numj;
  A+=((float)i)*numj;
  B+=((float)(i*i))*numj;
  coeff=-0.5;

 }

}else{

 for(i=0;i<=max-1;i++){

  numj=dta[i][3];
  N+=numj;
  A+=((float)i)*numj;
  B+=((float)(i*i))*numj;
  coeff=0.5;

 }

}

V_50=lowv+deltv*(A/N+coeff);
```

```
stdev=1.62*deltv*((N*B-(A*A))/(N*N)+0.029);

/*****************************************************************************/
/***PRINT RESULTS OF STATISTICAL ANALYSIS TO SCREEN**************************/
/*****************************************************************************/

printf("\nRESULTS OF STATISTICAL ANALYSIS:\n");
printf("Number of discrete voltage levels=%d\n",max);
printf("Total number of shots=%d\n",(int)numsh);
printf("Number of breakdowns=%d\n",(int)numbd);
printf("Number of withstands=%d\n",(int)numws);
printf("Delta voltage=%1.2f kV\n",deltv);
printf(" Vo=%3.2f kV\n V_50=%3.2f kV\n stdev=%2.2f kV\n\n",lowv,V_50,stdev);

}

float comp(one,two)
float one,two;

{
 float choose;

 if(one<two)

  choose=0.0;

 else

  choose=1.0;

 return choose;

 }
```